

See discussions, stats, and author profiles for this publication at: <https://www.researchgate.net/publication/5867851>

# New Novobiocin Analogues as Antiproliferative Agents in Breast Cancer Cells and Potential Inhibitors of Heat Shock Protein 90

ARTICLE *in* JOURNAL OF MEDICINAL CHEMISTRY · DECEMBER 2007

Impact Factor: 5.45 · DOI: 10.1021/jm0707774 · Source: PubMed

CITATIONS

87

READS

46

8 AUTHORS, INCLUDING:



Jean-François Peyrat

Université Paris-Sud 11

79 PUBLICATIONS 1,472 CITATIONS

SEE PROFILE



Mouâd Alami

French National Centre for Scientific Research

219 PUBLICATIONS 3,563 CITATIONS

SEE PROFILE



Barbara Stella

Università degli Studi di Torino

38 PUBLICATIONS 1,050 CITATIONS

SEE PROFILE



Jack-Michel Renoir

Institut de Cancérologie Gustave Roussy

125 PUBLICATIONS 5,063 CITATIONS

SEE PROFILE

## New Novobiocin Analogues as Antiproliferative Agents in Breast Cancer Cells and Potential Inhibitors of Heat Shock Protein 90

Gaëlle Le Bras,<sup>§,†</sup> Christine Radanyi,<sup>†,‡</sup> Jean-François Peyrat,<sup>§</sup> Jean-Daniel Brion,<sup>§</sup> Mouâd Alami,<sup>\*,§</sup> Véronique Marsaud,<sup>†</sup> Barbara Stella,<sup>†</sup> and Jack-Michel Renoir<sup>†</sup>

University of Paris-Sud, CNRS, BioCIS-UMR 8076, Laboratoire de Chimie Thérapeutique, and University of Paris-Sud, CNRS, UMR 8612, Laboratoire de Pharmacologie Cellulaire et Moléculaire des Anticancéreux, Faculté de Pharmacie, IFR 141, 5 rue J.-B. Clément, Châtenay-Malabry, F-92296, France

Received June 29, 2007

Selective hsp90 inhibitors simultaneously destabilize and deplete key signaling proteins involved in cell proliferation and survival, angiogenesis, and metastasis. Investigation of novobiocin analogues lacking the noviose moiety as novel inhibitors of hsp90 was carried out. A novel series of 3-aminocoumarin analogues has been produced and screened in cell proliferation, and the molecular signature of hsp90 inhibition was assessed by depletion of estrogen receptor, HER2, Raf-1, and cdk4 in human breast cancer cells. This structure–activity relationship study highlights the crucial role of the C-4 and/or C-7 positions of coumarin which appeared to be essential for degradation of hsp90 client proteins. Removal of the noviose moiety in novobiocin together with introduction of a tosyl substituent at C-4 or C-7 coumarins provides **6e** and **6f** as lead structures which compared favorably with novobiocin as demonstrated by enhanced rates of cell death. The processing and activation of caspases 7 and 8 and the subsequent cleavage of PARP by **6e** suggest stimulation of the extrinsic apoptosis pathway.

### Introduction

Heat shock protein 90 (hsp90) is a molecular chaperone that regulates the folding and maintains the proper conformation of many client proteins, the number of which is dramatically increasing and currently exceeds 150.<sup>1</sup> Of these hsp90 client proteins, steroid receptors, transcription factors, mutant p53, Hif-1 $\alpha$ , soluble kinases (Akt, Raf-1), transmembrane kinases (Her-2), and cdk-4 protein kinase<sup>2</sup> are directly associated with all six hallmarks of cancer.<sup>3</sup> Consequently, hsp90 has become an exciting new target in cancer drug discovery because the inhibition of its activity leads to depletion of these client proteins *via* the ubiquitin–proteasome pathway, thereby providing a simultaneous combinatorial attack on all the hallmarks of phenotypic cancer cells.

Hsp90 is an ATP-dependent protein which contains two nucleotide-binding sites. The N-terminal ATP binding domain binds the natural products geldanamycin **1**, radicicol **2** and their derivatives, and purine-, pyrazole-, and imidazopyrazine-based small molecule synthetic compounds.<sup>4</sup> Recent works demonstrated that novobiocin **3** (Nvb), a coumarin-containing DNA gyrase inhibitor, binds to hsp90 at the C-terminal nucleotide-binding region (Figure 1).<sup>5</sup> Inhibition of hsp90 by Nvb **3** leads to a decrease in hsp90 client proteins in various cancer cell lines,<sup>6</sup> an effect that is similar to N-terminal inhibitors, geldanamycin **1** and radicicol **2**.<sup>7</sup> Unfortunately, the ability of Nvb to induce degradation of hsp90 client proteins (e.g., ErbB2 in SkBr3 breast cancer cells)<sup>6</sup> is relatively weak ( $\sim 700 \mu\text{M}$ ) and requires further investigation to provide more potent compounds. To our knowledge, only two reports deal with the synthesis of active hsp90 inhibitors analogues related to Nvb **3**. In these structure–activity relationship (SAR) studies, Blagg et al.<sup>8a</sup> have highlighted the crucial role of the noviose moiety at the

7-position of the coumarin ring for the biological activity and showed that compound **4a** without the 4-hydroxyl of the coumarin moiety and containing an *N*-acetyl side chain in lieu of the benzamide was the most active compound (Figure 1). More recently in continuation of their structural modification studies, Blagg et al.<sup>8b</sup> reported that 3'-descarbamoyl-4-deshydroxynovobiocin **4b** proved to be a more effective and selective hsp90 inhibitor (degradation of ErbB2 and p53 between 0.1 and 1.0  $\mu\text{M}$ ). Although analogues **4** containing both modified sugar and coumarin moieties revealed higher potency than Nvb itself to induce client-proteins loss, the design of novel more potent hsp90 inhibitors is still presently of great importance.

As part of our research field concerning hsp90,<sup>9</sup> we initiated a research program aimed at identifying novel inhibitors based on nonsugar coumarin scaffold. In order to establish a SAR profile on this hsp90 targeting agent, we have synthesized a series of novobiocin analogues of general structure **A** lacking the noviose moiety including those that connect the substituted coumarin ring to the aryl moiety through an amide, a retroamide, and an alkyne linkage. Furthermore, the triple bond in these compounds would provide a focal point for further structural manipulation. For instance, hydration would lead to new analogues having a ketone function instead of an amide linker.

The potencies of newly synthesized novobiocin derivatives lacking the noviose moiety were evaluated using several biological assays including cell proliferation and flow cytometry as well as their capacity to induce the proteasome-mediated degradation of HER2 (also known as ErbB2/Neu), Raf-1, cdk4, and estrogen receptor (ER<sup>a</sup>) and to inhibit estradiol (E<sub>2</sub>)-induced transcription in human breast cancer cells. Among the synthetic derivatives, compounds **6c**, **6e**, and **6f** showed the most potent inhibitory activity against the proliferation of MCF-7 human

\* To whom correspondence should be addressed. Phone: 33 (0)1.46.83.58.87, fax: 33(0)1.46.83.58.28, e-mail: mouad.alami@u-psud.fr.

<sup>§</sup> Univ Paris-Sud, CNRS, BioCIS-UMR 8076.

<sup>†</sup> Univ Paris-Sud, CNRS, UMR 8612.

<sup>‡</sup> Contributed equally to this work.

<sup>a</sup> Abbreviations: ER, estrogen receptor; E<sub>2</sub>, estradiol; PARP, poly(ADP-ribose) polymerase; LUC, luciferase; TCEs, total cell extracts; ERE, estrogen responsive element; DMEM, Dulbecco's modified eagle medium; FCS, fetal calf serum; SDS-PAGE, SDS-polyacrylamide gel electrophoresis; PI, propidium iodide.

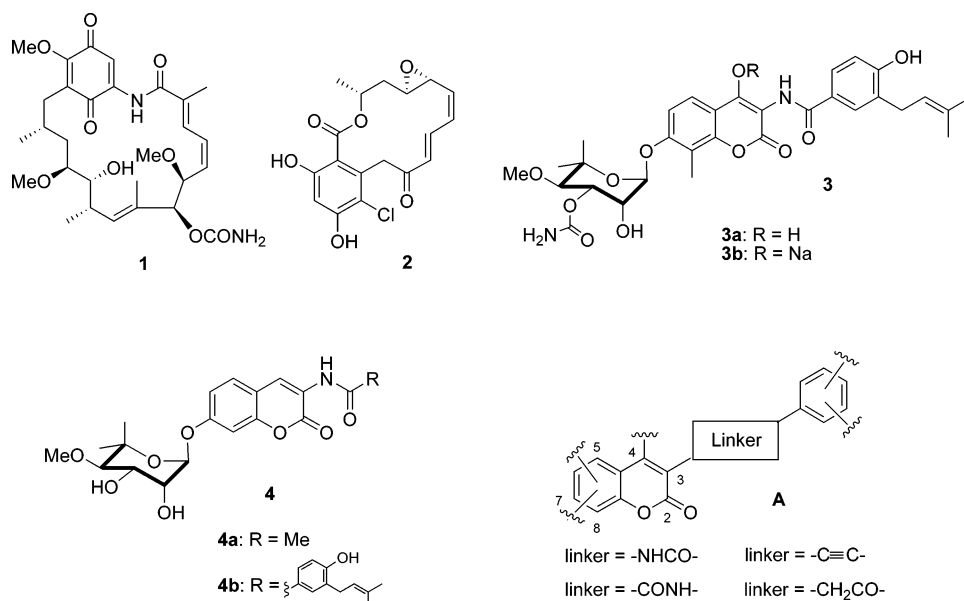
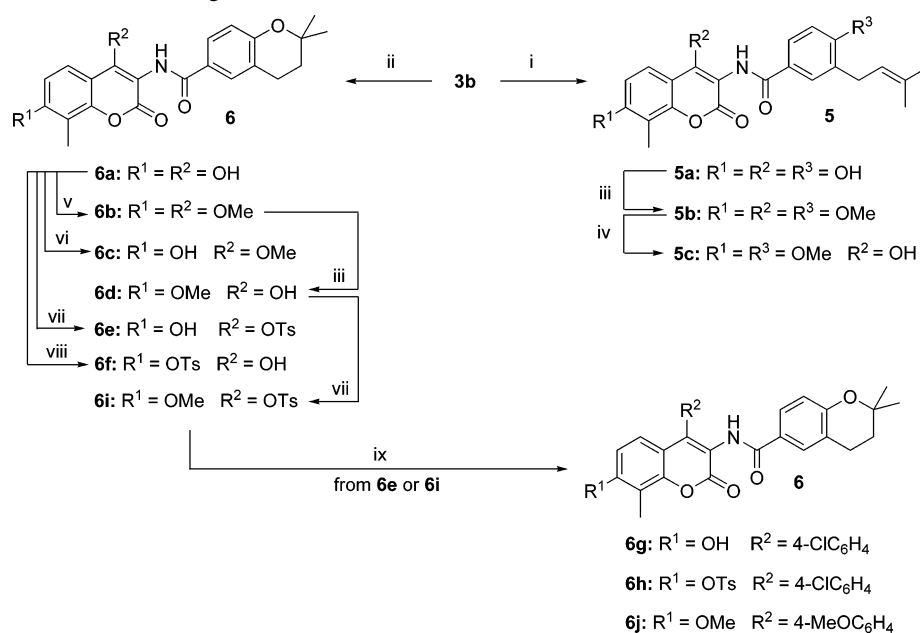


Figure 1. Hsp90-inhibitors 1–4 and general structure A of the synthesized compounds.

### Scheme 1. Denoviose Novobiocin Analogues<sup>a</sup>



<sup>a</sup> Reagents and conditions: (i) AcCl (2 equiv), EtOH, 78 °C, 2 h; (ii) 12 N HCl/H<sub>2</sub>O, 78 °C, 1 h; (iii) Me<sub>2</sub>SO<sub>4</sub>, K<sub>2</sub>CO<sub>3</sub>, DMF, rt, 16 h; (iv) morpholine, MeOH, reflux, then 1 N HCl/H<sub>2</sub>O; (v) Me<sub>2</sub>SO<sub>4</sub>, K<sub>2</sub>CO<sub>3</sub>, DMF-acetone, rt, 16 h; (vi) Me<sub>2</sub>SO<sub>4</sub> (1.1 equiv), K<sub>2</sub>CO<sub>3</sub>, DMF, rt, 48 h; (vii) TsCl, pyridine, rt; (viii) TsCl, DMAP, Et<sub>3</sub>N, THF, rt; (ix) ArB(OH)<sub>2</sub>, K<sub>3</sub>PO<sub>4</sub>, PdCl<sub>2</sub>(dppf), MeCN, 80 °C.

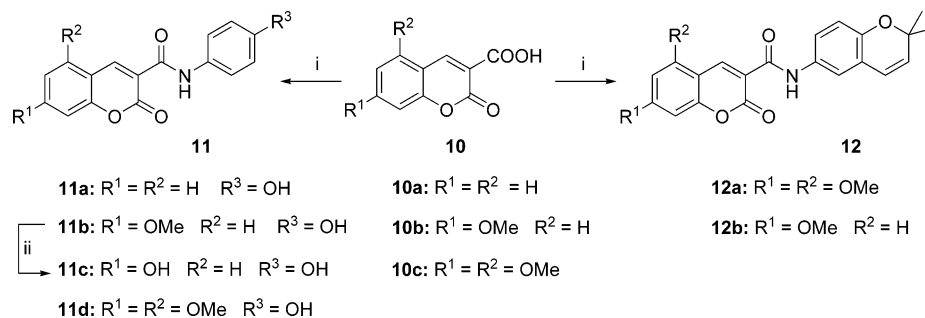
breast cancer cells. The synthesis, structure determination and hsp90 inhibiting activity of these novobiocin analogues will be described.

### Results and Discussion

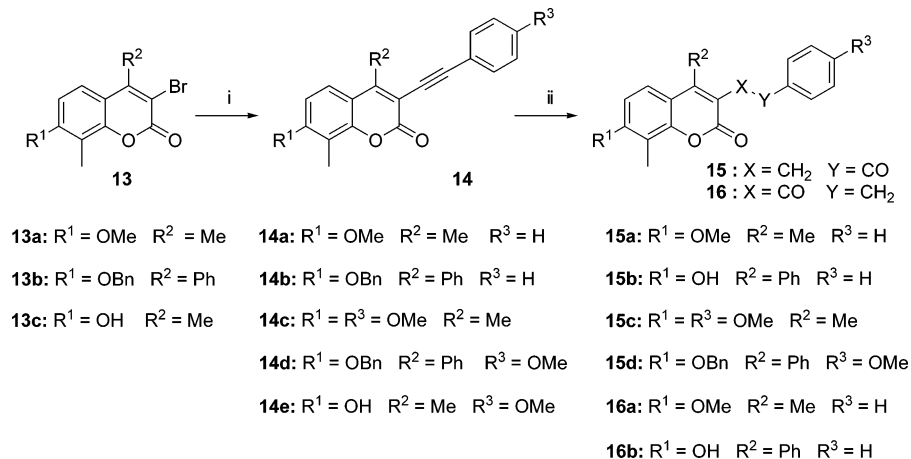
**Synthesis of Novobiocin Analogues.** The target structures 5 and 6 with an amide linkage were prepared by acidic hydrolysis of monosodium novobiocin salt<sup>10</sup> readily available from Sigma-Aldrich (Scheme 1). Thus, treatment of 3b with 2 equiv of acetyl chloride in boiling absolute ethanol yielded novobiocic acid 5a while in the presence of an excess of concentrated hydrochloric acid, a quantitative yield of cyclonovobiocic acid 6a was obtained. Subsequent methylation of free hydroxyl groups using an excess of dimethyl sulfate and K<sub>2</sub>CO<sub>3</sub> in DMF gave methylated derivatives 5b and 6b in 62%

and 61% isolated yield, respectively. During the course of these studies, it was observed that the methylation reaction was less successful when using methyl iodide instead of dimethyl sulfate. Thus, reaction of cyclonovobiocic acid 6a with an excess of methyl iodide (5 equiv) in the presence of K<sub>2</sub>CO<sub>3</sub> was sluggish and gave a mixture of two compounds 6b and 6c, which were easily separated by chromatography on silica gel.

For the synthesis of the corresponding analogues 5c and 6d having a free 4-hydroxyl group, we planned to selectively cleave the methoxy group in the C-4 position of the coumarin ring under acidic conditions, as it could be regarded as a vinylagous ester. Thus, attempted conversion of 6b to 6d in the presence of aqueous hydrochloric acid solution was unsuccessful and starting material was recovered unchanged. However, we found that when compound 6b was treated with morpholine in boiling

**Scheme 2.** Denoviose Novobiocin Analogues with a Retroamide Linkage<sup>a</sup>

<sup>a</sup> Reagents and conditions: (i) ArNH<sub>2</sub>, PyBOP, DIEA, DMF, rt; (ii) pyridinium chloride, 160 °C.

**Scheme 3.** Denoviose Novobiocin Analogues with an Acetylenic or a Carbonyl Linkage<sup>a</sup>

<sup>a</sup> Reagents and conditions: (i) ArC≡CH, PdCl<sub>2</sub>(PPh<sub>3</sub>)<sub>2</sub>, PPh<sub>3</sub>, CuI, Et<sub>3</sub>N, dioxane, 100 °C sealed tube; (ii) PTSA, EtOH, microwave, 120 °C or 170 °C, 0.5 h.

methanol followed by acidic hydrolysis, it efficiently provided 4-hydroxycoumarin derivative **6d** in good yields. In a similar way, compound **5b** gave the corresponding derivative **5c**.

In order to evaluate the importance of the free 4-hydroxyl group in derivatives **6**, we planned to introduce an aryl substituent by metal-catalyzed cross-coupling reaction. For this purpose, the use of aryl tosylates as electrophiles for the Suzuki-type coupling is a very attractive procedure.<sup>11</sup> The synthesis of the required 4-tosylcoumarin **6e** was attempted from dihydroxycoumarin **6a** using tosyl chloride in the presence of DMAP and triethylamine in THF. Under these conditions, the tosylation reaction proceeded smoothly and occurred selectively at the 7-hydroxyl position to give compound **6f**. However, when the reaction was run in pyridine, we were pleased to observe selectively the 4-hydroxyl tosylation leading to the required 4-tosylcoumarin **6e**. Under similar conditions, tosylcoumarin **6i** was obtained from **6d**. Compound **6e** having a free 7-hydroxyl group was then submitted to cross-coupling with 4-chlorophenylboronic acid. Thus several reported Suzuki conditions were examined using various combinations of Pd/solvent/bases (e.g., Pd(PPh<sub>3</sub>)<sub>4</sub>, Pd(OAc)<sub>2</sub>, PdCl<sub>2</sub>(PPh<sub>3</sub>)<sub>2</sub>, PdCl<sub>2</sub>(dppf)/ MeCN, THF, DME/K<sub>2</sub>CO<sub>3</sub>, Cs<sub>2</sub>CO<sub>3</sub>, Na<sub>2</sub>CO<sub>3</sub>). Contrary to expectations, we found that optimal conditions (K<sub>3</sub>PO<sub>4</sub>, PdCl<sub>2</sub>(dppf), MeCN, 80 °C, 2.5 h) did not afford compound **6g** but rather allows the formation of the coupling product **6h** having a tosyl substituent at the 7-hydroxyl position. Under similar conditions, performing the Suzuki coupling reaction from 4-tosylcoumarin **6i** with 4-methoxyphenylboronic acid furnished the coupling product **6j** in excellent yield.

The syntheses of novobiocin analogues **11** and **12** having a retroamide linkage began with the preparation of known

compounds **10**<sup>12</sup> (Scheme 2). Further amidification with a series of anilines in the presence of PyBOP and DIEA in DMF at room-temperature gave the target structures **11** and **12** in good yields. Because of the strong insolubility of these derivatives in the usual organic solvents, we examined the methoxy cleavage only on derivatives **11**. Thus, treatment of **11d** with pyridinium chloride resulted in complex mixtures of nonidentified products while under similar conditions **11b** afforded the corresponding 7-hydroxy analogue **11c** in a reasonable yield.

As shown in Scheme 3, acetylenic novobiocin analogues **14** having a carbon–carbon triple bond linkage were prepared by the palladium-mediated Sonogashira–Linstrumelle (S–L) coupling reaction of terminal alkynes with substituted 3-bromocoumarins **13**.<sup>13</sup> It should be noted that this coupling reaction is well-known to be sluggish with brominated derivatives **13** and often requires specific conditions<sup>14</sup> according to the nature and the position of substituents. Thus, for the coupling of phenyl- or 4-methoxyphenylacetylene with 7-OMe or 7-OBn bromocoumarin derivatives substituted in C-4 position, the use of CuI (10 mol %) as cocatalyst in combination with PdCl<sub>2</sub>(PPh<sub>3</sub>)<sub>2</sub> (20 mol %), and PPh<sub>3</sub> (20 mol %) in dioxane in a sealed tube at 100 °C resulted in optimal conditions. Accordingly, reaction from **13b** resulted in **14b** and **14d** in moderate to good yields. In a similar way, coupling of bromocoumarin **13a** gave **14a** and **14c**. One can note that under these conditions, the coupling reaction of **13c** having a free 7-hydroxyl group did not go to completion and lead to a mixture of inseparable **13c** and **14e**.

Finally, the synthesis of analogues **15** with a ketone function was achieved by hydration of analogous acetylenic compounds according to our previously reported method.<sup>15</sup> Thus, microwave-

**Table 1.** Growth Inhibitory Activity of Novobiocin Analogues in MCF-7 Cells

compound	IC <sub>50</sub> (μM)
<b>5a</b>	170
<b>5b</b>	NE <sup>a</sup>
<b>5c</b>	90
<b>6a</b>	>200 <sup>b</sup>
<b>6b</b>	>200 <sup>b</sup>
<b>6c</b>	40
<b>6d</b>	>200 <sup>b</sup>
<b>6e</b>	50
<b>6f</b>	75
<b>6h</b>	NE <sup>a</sup>
<b>6i</b>	55
<b>6j</b>	NE <sup>a</sup>
Nvb	260

<sup>a</sup> NE = no effect at 200 μM. <sup>b</sup> 75% viable cells at 200 μM. For assay conditions, see Experimental Section.

assisted hydration was first examined with substrates **14a** and **14b** bearing a nonactivated aryl ring in the presence of *p*-toluenesulfonic acid in boiling alcoholic media at 170 °C for 2 h. Under these conditions, hydration reaction of 7-OBn acetylenic coumarin **14b** occurred together with deprotection of the benzyl ether group and gave a 1/1 mixture of nonseparable regioisomers **15b** and **16b**. Similarly, hydration of acetylenic compound **14a** furnished a 75/25 mixture of **15a** and **16a** which were in this case easily separable by chromatography. We next examined the hydration of substrates with an activated aryl ring. We were pleased to observe that **14c** and **14d** derivatives having a *p*-methoxyphenyl group underwent successfully and regioselectively the hydration reaction at a lower temperature (120 °C) leading to the corresponding carbonyl compounds **15c** and **15d**, respectively.

## Biological Results

**Cytotoxicity.** Since all the novobiocin analogues from series **5** and **6** were soluble in DMSO at concentrations high enough to allow cell experiments, the *in vitro* biological activity of these analogues was first evaluated by their growth-inhibitory potency in MCF-7 human breast cancer cells. Data presented in Table 1 showed that unlike **5b**, **6h**, and **6j** which displayed no effects, compounds **5c**, **6c**, **6e**, and **6f** having one free 4- or 7-hydroxyl group exhibited improved growth inhibition potentials as compared to the parent compound. Replacement of the prenyl benzoate natural product in **5c** with 2,2-dimethyl-2H-chromane moiety in **6d** resulted in decreased growth inhibitory activity. Derivatives **6a** and **6b** having on C-4 and C-7 positions of coumarin both hydroxyl groups free or substituted by a methyl group were much less active than Nvb **3** since they only slightly affected the growth of MCF-7 cells (75% survival) even at the highest tested concentration (200 μM). Moderate cell uptake due to precipitation or poorer permeability of these compounds into cells as well as rapid metabolism or increased drug efflux could account for their low potencies in growth inhibitory assay. Alternatively, retention within cells could be altered due to adsorption of the drugs to the plastic surfaces of the culture dishes or binding to serum proteins or other cellular proteins thus reducing specific binding to hsp90. These hypotheses will be discussed below.

**Flow Cytometry.** All the soluble novobiocin analogues were evaluated by flow cytometry analysis. As shown in Table 2, all the compounds except **5b** and **6h** affected the progression of MCF-7 cells in the cell cycle, although at different phases and to various extent. The percentage of cells in the G<sub>0</sub>/G<sub>1</sub> phase was moderately increased by treatment of cells with derivatives

**Table 2.** Flow Cytometry Analysis of Novobiocin Analogues in MCF-7 Cells<sup>a</sup>

compound	cell cycle							
	48 h				72 h			
	SubG1	G <sub>0</sub> /G <sub>1</sub>	S	G <sub>2</sub> /M	SubG1	G <sub>0</sub> /G <sub>1</sub>	S	G <sub>2</sub> /M
DMSO	2.9	70.7	17.7	10.7	3.6	76.4	14.9	7.6
Nvb	5.9	59.9	19.7	19.3	9.8	58.3	21.3	19.3
<b>5a</b>	4.8	28.0	29.0	42.6	6.1	24.3	17.0	58.5
<b>5b</b>	3.6	73.3	14.4	10.8	3.8	82.1	10.2	6.9
<b>5c</b>	2.8	70.1	17.3	9.8	3.0	83.2	9.8	5.9
<b>6a</b>	7.7	46.5	36.2	14.4	6.0	58.1	23.4	18.6
<b>6b</b>	7.5	56.7	28.4	11.9	3.8	77.8	14.8	7.2
<b>6c</b>	7.7	57.7	27.1	13.5	17.0	65.1	22.7	9.5
<b>6d</b>	3.3	71.9	16.2	10.7	2.5	85.4	8.5	6.5
<b>6e</b>	28.8	53.6	23.1	20.6	43.2	57.2	22.7	18.4
<b>6f</b>	7.1	22.5	25.9	51.0	8.6	14.6	13.3	71.6
<b>6h</b>	3.8	70.4	19.7	9.9	4.9	74.1	17.1	7.5
<b>6i</b>	2.9	81.2	9.3	8.0	3.4	84.0	6.7	8.6
<b>6j</b>	3.7	71.0	15.3	11.5	4.0	81.3	9.5	7.7

<sup>a</sup> Data represent percentage of cells in each phase of the cell cycle. The results are the mean of two independent experiments in which no more than 2.5% variations were measured.

**5c**, **6d**, **6i**, and **6j** as compared with vehicle-treated asynchronously growing cells. The G<sub>0</sub>/G<sub>1</sub> block was accompanied by a decline in the S and G<sub>2</sub>/M phases of the cell cycle. Treatment with derivatives **6a**, **6c**, and **6e** led to a slight accumulation of cells in the S phase while compound **6b** enhanced the percentage of cells in the S phase at 48 h and G<sub>0</sub>/G<sub>1</sub> at 72 h. A more pronounced accumulation of cells in the G<sub>2</sub>/M phase and a corresponding strong reduction of the G<sub>0</sub>/G<sub>1</sub> population were observed in cells exposed to **5a** and **6f** as compared to Nvb. Increasing the incubation time to 72 h substantially increased the percentage of cells arrested in G<sub>2</sub>/M. Compounds **5a**, **6a**, and **6f** also induced a weak apoptosis similarly to Nvb. On the contrary, compounds **5b**, **5c**, **6b**, **6d**, **6h**, **6i**, and **6j** had no effect on apoptosis thus ruling out nonspecific cell-killing. Importantly, derivatives **6c** and **6e** strongly triggered sustained apoptosis of MCF-7 cells (8 and 29% at 48 h increasing to 17 and 43% at 72 h, respectively). Altogether these results indicate that every analogue appears to induce different cell-cycle arrest phenotype with different extent of cell death. The stage of cell cycle block or induction of apoptosis by hsp90 inhibitors, including a selection of purines, radicicol, and 17-AAG has been reported to be cell line- and tumor type-dependent.<sup>16</sup> In addition, hsp90 exerts pleiotropic role in chaperoning several cell cycle regulatory proteins, including those involved in G<sub>0</sub>/G<sub>1</sub> and G<sub>2</sub>/M entry, and its activity is regulated by the stepwise recruitment of cochaperones (e.g., immunophilins, cdc37, p23).<sup>17</sup> Selective affinities or binding to distinct regions on hsp90 leading to depletion of different key signaling proteins involved in pathways regulating cell proliferation and survival might explain the different effects of our novobiocin analogues. There is now accumulating evidence that hsp90 inhibitors and cochaperones induce structural and conformational changes within multiple regions of the protein.<sup>7a,18</sup> Moreover, Nvb is able to compete with both geldanamycin- and radicicol-affinity beads for binding of hsp90<sup>6</sup> and interferes with the interaction between the cochaperones p23 and cdc37 and the N-terminal domain of hsp90.<sup>5,19</sup> It seems conceivable that upon binding novobiocin derivatives harboring new functionalities, hsp90 could undergo conformational changes leading to disruption of discrete subcomplexes associated with partner proteins or clients which may be accompanied by cell cycle arrest in different locations. The weak or strong growth inhibitory activity of novobiocin analogues (Table 1) correlated with their ability to slightly or



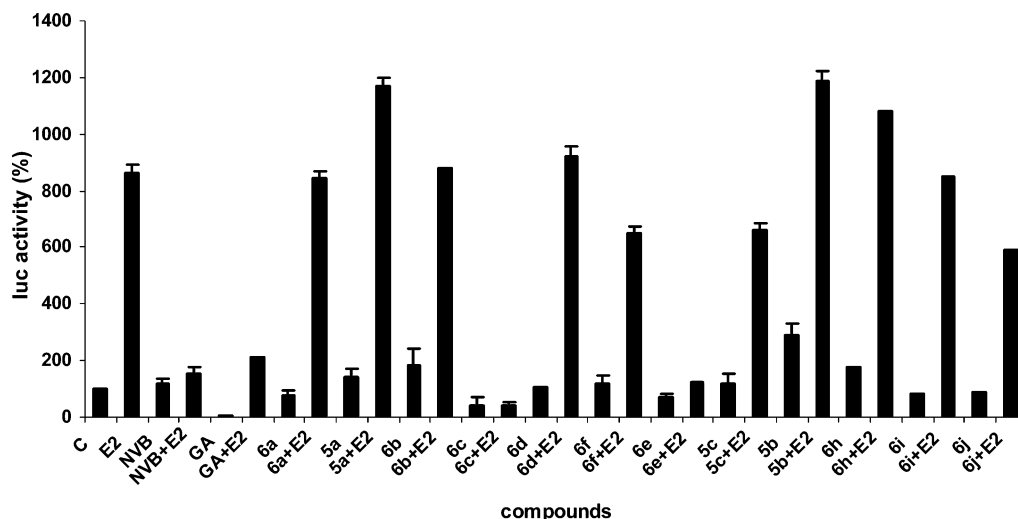


**Figure 2.** Capacity of novobiocin analogues to affect ER-mediated transcription in breast cancer cells. MELN cells were cultured and treated with the different hsp90 inhibitors (GA = 2  $\mu$ M; Nvb and analogues = 200  $\mu$ M) as described in Experimental Section and then exposed or not for 18 h to 0.1 nM E<sub>2</sub>. LUC was measured and the level of LUC activity expressed as a function of the different treatments as the mean  $\pm$  SEM of two independent experiments performed in triplicate, 100% being affected to the basal transcription level obtained with vehicle only (C).

markedly affect cell cycle and/or induce cell cycle arrest or apoptosis, respectively.

**Capacity of Novobiocin Analogues To Inhibit E<sub>2</sub>-Induced Transcription in MELN Cells.** As shown in Figure 2, the E<sub>2</sub>-increased luciferase (LUC) activity in MELN cells reaches 9-fold that of the basal LUC activity; exposure to GA completely abolished both the basal and E<sub>2</sub>-induced transcriptional response whereas Nvb did not affect basal transcription but strongly inhibited the E<sub>2</sub>-induced transactivation capacity of ER as previously observed.<sup>9b</sup> In the MELN cells used, the novobiocin analogues affected transcription differently; these analogues can be classified as follows: (i) those which had no marked or weak effects on LUC activity (like **5c**, **6a**, **6b**, **6d**, **6f**, **6i**, and **6j**); (ii) those which slightly enhanced LUC activity (like **5a**, **5b**, and **6h**); (iii) those which strongly inhibited both the basal and E<sub>2</sub>-induced LUC activity (like **6c** and **6e**). Note that when E<sub>2</sub> is added first, compound **6e** does not affect LUC expression (not shown) thus supporting a direct inhibitory activity on hsp90 in agreement with an E<sub>2</sub>-induced ER-hsp90 complex dissociation.<sup>1a, 9b</sup>

**Proteasome-Mediated ER $\alpha$  Degradation.** Given that inhibition of hsp90 leads to a proteasome-mediated degradation of client proteins, and since ER belongs to the family of transcription factors which are hsp90-client proteins, we further wondered if the various novobiocin analogues **5** and **6** could affect the stability of ER. MCF-7 cells were exposed to the analogues following or not 30 min incubation with MG132, a peptide aldehyde inhibitor of the catalytic unit of the proteasome. Nvb and 17-allylamino-17-demethoxygeldanamycin (17AAG) were used as positive controls. Among the novobiocin analogues tested (Figure 3A), **6c**, **6e**, **6f**, and **6i** were able to induce a loss of ER $\alpha$  protein, suggesting inhibition of hsp90 and disruption of heteroprotein complexes. It is interesting to note that as shown in the growth inhibitory assay and flow cytometric analysis, derivatives **6e** and **6f** exhibited higher potency to induce ER $\alpha$  down-regulation than Nvb. In addition, ER $\alpha$  was difficult to detect in lysates of cells treated with **6c**, **6f**, and **6e** both in the presence and the absence of the proteasome inhibitor MG132. This feature could be explained by a relocation of destabilized ER in a detergent-resistant cell compartment which, in turn, could be less accessible to proteasome inhibitors. In fact,

in total cell extracts (TCEs) from similarly treated cells, MG132 blocked the drug-induced receptor degradation (Figure 3B) suggesting that proteasome-mediated proteolysis of ER $\alpha$  likely occurs in a compartment from which the receptor is not extractable by conventional lysis buffers as reported for pure antagonists-promoted ER degradation.<sup>20</sup> The potency of compounds **6c** and **6e** to down-regulate ER $\alpha$  correlated well with the inhibition of E<sub>2</sub>-induced LUC gene expression. By contrast, the other novobiocin analogues which failed to inhibit LUC expression (Figure 2) were also unable to induce ER $\alpha$  destabilization (Figure 3). These results also indicated that analysis of E<sub>2</sub>-induced transcription in MELN cells represents a fast, highly reproducible and functional assay for the initial screening of a library of hsp90 inhibitors. The analogue **6e** appeared as one of the most powerful compounds since processing of ER $\alpha$  occurred over a range of 5–200  $\mu$ M (Figure 3C, upper panel). Densitometric analysis of signals corresponding to ER $\alpha$  indicated 23, 34, and 46% decrease at 5, 10, and 20  $\mu$ M **6e**, respectively, as compared to vehicle-treated extracts (not shown). By comparison compound **6f** was nearly as potent as visualized by degradation of ER $\alpha$  over a range of 20–200  $\mu$ M (Figure 3C, lower panel). In addition, the analogue **6e** promoted a strong and sustained loss of ER $\alpha$  since even at 72 h, ER $\alpha$  did not return to basal level (Figure 3D). This result is consistent with the sustained cell death promoting effect of **6e** reported in Table 2. To check for drug stability and/or binding to serum proteins as well as adsorption to plastic surfaces which could result in reduction of both binding and consequent inhibition of hsp90, we proceeded with two additional experiments. First, compound **6e** was preincubated for 24 h at 37  $^{\circ}$ C in culture medium prior to addition to cultured cells and further analysis of ER $\alpha$  down-regulation. From the results depicted in Figure 3E full degradation of ER $\alpha$  was achieved at higher concentration (200  $\mu$ M) than that observed following direct exposure to **6e** (50  $\mu$ M). Second, in experiment conducted in the presence of 0.1% FCS, ER $\alpha$  did not undergo destabilization at lower concentrations of **6e** (data not shown) thus ruling out degradation by and/or binding to serum components. Therefore, and given that our novobiocin analogues share similar structures, one can assume that partial adsorption of the more active drugs to plastic

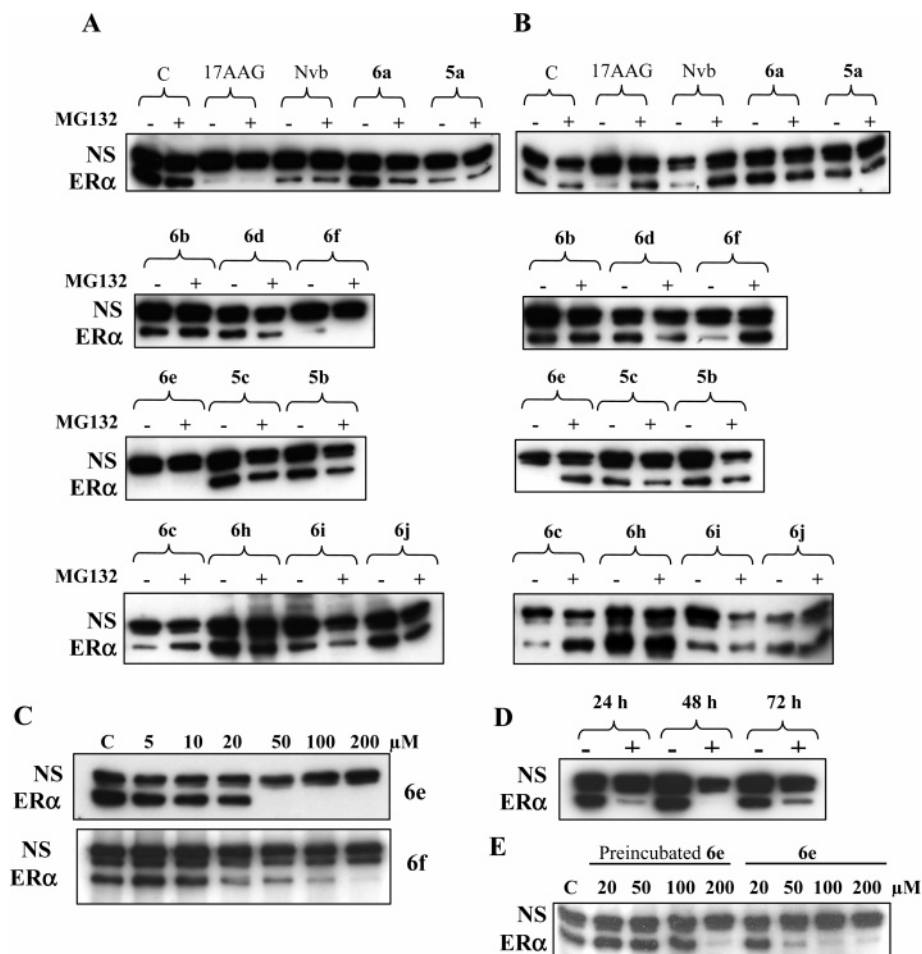


**Figure 3.** Effects of novobiocin analogues on ER $\alpha$  stability. MCF-7 cells were grown and exposed to hsp90 inhibitors (17AAG, 2  $\mu$ M; Nvb and analogues, 200  $\mu$ M) as described in Experimental Section in the presence (+) or absence (–) of the proteasome inhibitor MG132 (5  $\mu$ M) added 30 min prior drug treatment. (A) Cell lysates and (B) TCEs (20  $\mu$ g protein) were analyzed by Western blotting with D12 anti ER $\alpha$  antibody. C = control cell lysates exposed to vehicle only, NS = nonspecific protein band detected in these conditions and serving as a control of constant protein loading. (C) Dose–response of ER $\alpha$  fate following exposure of MCF-7 cells to increasing concentrations of **6e** (upper panel) or **6f** (lower panel) for 16 h. Cells were cultured and treated, and cell lysates were analyzed as above. (D) Degradation kinetic of ER $\alpha$  from MCF-7 cells following exposure (+) or not (–) to **6e**. The cells and lysates were prepared as above after treatment for the indicated time with 100  $\mu$ M of **6e**. (E) Dose–response of ER $\alpha$  degradation following exposure of MCF-7 cells to **6e** preincubated in DMEM for 24 h or direct exposure to **6e**. NS = nonspecific protein band serving as a control of constant protein loading.

surfaces appears likely and accounts for their apparent low potencies in biological assays.

**Effects of Novobiocin Derivatives on hsp90-Dependent Signaling Proteins.** The potency of novobiocin analogues was further assessed in MCF-7 cells by the depletion of HER2, Raf-1, and cdk4, the most widely studied molecular signatures indicative of hsp90 blockade. Following exposure for 18 h, 17AAG and Nvb decreased HER2 expression (Figure 4) as already reported.<sup>7c,16c,21</sup> Among the novobiocin analogues, compounds **6c**, **6e**, **6f**, and to a lesser extent **5b** and **5c** also decreased the steady-state level of HER2 (Figure 4). Proteasome inhibition induced by MG132 did not result in accumulation of HER2, but this observation is not intriguing in light of recent report showing an association between reduction in proteasome activity by bortezomib and degradation and loss of ErbB2 function.<sup>22</sup> We next examined the effects of the drugs on the expression of Raf-1, a central player of the Ras-MAP kinase pathway. In addition to 17AAG and Nvb, compounds **5a**, **5c**, **6c**, **6e**, **6f**, and **6h** significantly decreased Raf-1 expression (Figure 4). Exposure of MCF-7 cells to drugs resulted in much less pronounced effects on cdk4 levels (Figure 4). In contrast to HER2 and Raf-1, 17AAG only partially depleted cdk4. In addition, given that Nvb was without effect, derivatives **6a**, **6e**,

and **6f** were more potent than the parent compound. As compared to vehicle-treated control cells, analogues **5b**, **5c**, **6c**, **6h**, **6i**, and **6j** induced a slight decline in cdk4 levels. Altogether these results are in agreement with previous studies showing that the various client protein kinases are not equally responsive to hsp90 inhibitors and sensitivity might depend on how each kinase interacts with hsp90 and the cochaperone cdc37.<sup>23</sup> For example, ErbB2 and Raf-1 bind to both hsp90 and cdc37 in a persistent manner and this makes them very sensitive targets of GA in contrast to cdk4 which interacts transiently with hsp90 immediately following translation and is therefore depleted more slowly following pharmacological inactivation of cdc37/hsp90 function.<sup>23,24</sup> Given that the degradation of HER2 and Raf-1 is now considered as a functional read-out of Hsp90 inhibition,<sup>4c</sup> the down-modulation of HER2, Raf-1, cdk4, and ER expression strongly supports disruption of heteroprotein complexes by novobiocin derivatives likely related to their ability to bind and inhibit hsp90. In addition, the simultaneous inhibition of the HER2/PI3kinase/Akt and Ras/Raf/MAP kinase pathways as well as cdk4 degradation likely translate to the potency of several novobiocin analogues for inhibiting cellular proliferation (Table 1) and inducing cell cycle arrest or apoptosis (Table 2). Therefore, we believe that these compounds may have hsp90

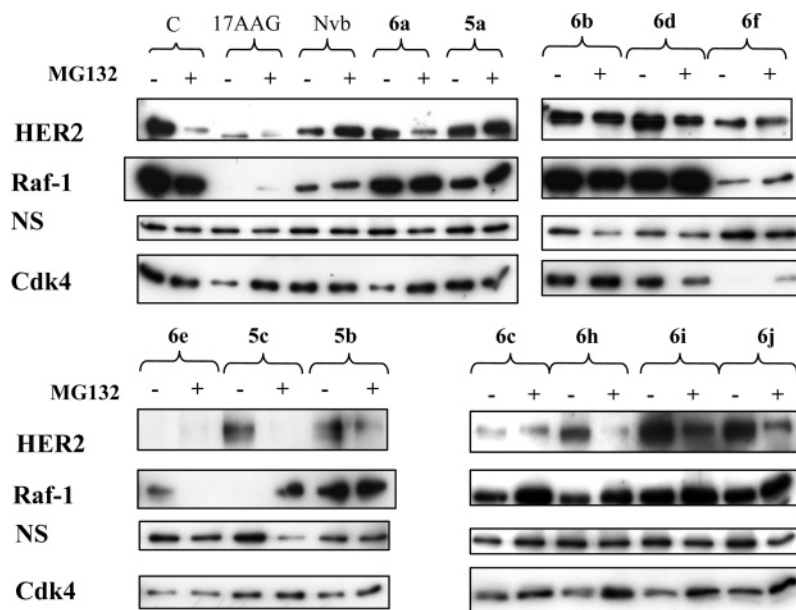


**Figure 4.** Effects of novobiocin analogues on client proteins stability. MCF-7 cells were exposed to drugs (17AAG, 2  $\mu$ M; Nvb and analogues, 200  $\mu$ M) in the presence (+) or absence (–) of MG132 (5  $\mu$ M) as in Figure 3. Cell lysates (20  $\mu$ g protein) were fractionated by SDS-PAGE at 12% acrylamide concentration (cdk4). A nonspecific protein (NS) is visualized and serves as an internal loading control. The membranes used for detection of ER $\alpha$  and NS signals described in Figure 3 were stripped as indicated in Experimental Section and sequentially reprobed with Raf-1 and HER2 antibodies.

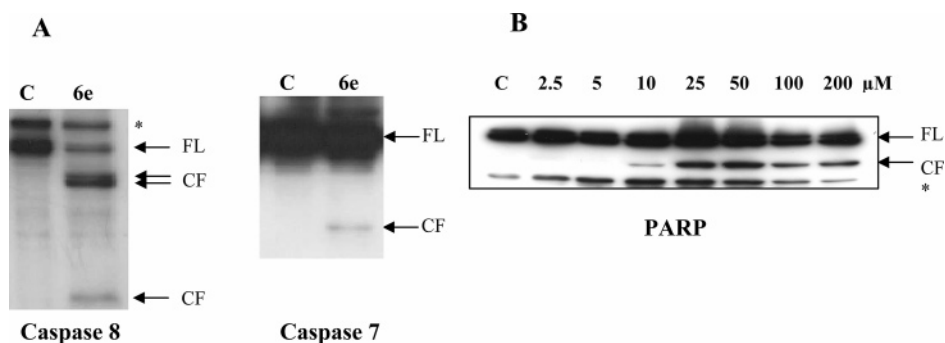


**Figure 5.** Effects of **6e** on caspase activation and PARP cleavage. (A) MCF-7 cells were cultured overnight with DMSO (C) or compound **6e** (200  $\mu$ M), and cell lysates (20  $\mu$ g protein) were fractionated by SDS-PAGE at 12% acrylamide concentration followed by Western blotting. (B) Dose-response of PARP cleavage following exposure of MCF-7 cells to increasing concentrations of **6e** for 16 h. Cell lysates were analyzed by SDS-PAGE at 8% acrylamide concentration and subjected to Western blot analysis using anti PARP antibody. Proteins reacting nonspecifically with antibodies are indicated (\*) and serve as internal loading controls. The arrows indicate the full length (FL) and cleaved fragment (CF) of caspases (p43/41 and p18 CF for caspase 8, respectively; p19 CF for caspase 7) and PARP.

specific cellular activity and that the cytotoxicity likely relates to hsp90 inhibition. Moreover, it must be emphasized that overexpression of HER2 in 30–40% of breast, ovarian, prostate, and non-small cell lung cancer is linked to enhanced resistance to chemotherapeutic drugs and poor prognosis, and only 35% of breast cancer patients demonstrate a clinical response to trastuzumab.<sup>25</sup> The Ras/Raf/MAP kinase signaling pathway is also found activated in ~30% of human cancer.<sup>26</sup> In addition, it is now well-established that increased growth factor and kinase signaling is a potent mechanism for the promotion of ER-dependent and-independent forms of antiestrogen resistance and aggressive behavior in breast cancer patients.<sup>27</sup>

**Caspase Involvement in 6e-Induced Apoptosis of MCF-7 Cells.** Flow cytometric analysis revealed that compound **6e** is a potent inducer of programmed cell death (Table 2), and we next examined the molecular mechanism underlying its effects. Apoptosis can be initiated by various means such as stimulation of cell surface death receptors upon specific ligand or antibody binding (extrinsic pathway), perturbation of mitochondrial function (intrinsic pathway) and triggering by autoactivation of

initiator caspases (e.g., 8 and 9) which in turn activate effector caspases (e.g., 3 and 7).<sup>28</sup> Although MCF-7 cells lack procaspase 3,<sup>29</sup> Liang et al. showed that in these cells the apoptotic pathway was able to proceed *via* sequential activation of caspase 9 followed by that of caspase 7 and 6.<sup>30</sup> Since caspase 7 can be activated by both intrinsic and extrinsic apoptotic pathways, we analyzed processing of caspase 9 and caspase 8, respectively. Upon exposure of MCF-7 cells to compound **6e** we found no evidence for caspase 9 activation (data not shown), but as shown in Figure 5A, a decline in full length caspase 8 expression level and accumulation of the cleaved intermediate p43/41 and the active subunit p18 were detected. Caspase 7 was processed to its active form in response to **6e** treatment as visualized by the apparition of the p19 subunit (Figure 5A). Since caspase-7 activation induces the cleavage of poly(ADP-ribose) polymerase (PARP),<sup>31</sup> we further wondered whether **6e** could trigger similar effects. A dose-dependent processing of the 116 kDa full length form of PARP to the cleaved fragment of 85 kDa over the range of 10–200  $\mu$ M occurred after treatment with **6e** (Figure 5B). This result correlated well with the growth inhibiting activity



of **6e** (Tables 1 and 2) and likely suggests that mitochondrial damage and hence caspase 9 were not involved in induction of apoptosis and rather supports stimulation of the extrinsic pathway.

Altogether, the data reported above suggest that novobiocin analogues lacking the noviose moiety and having a C-4 or C-7 tosyl substituent exhibit an increased capacity to inhibit hsp90. Indeed, compounds **6e** and **6f** appear more potent hsp90 inhibitors than Nvb. It should be noted that both analogues block hsp90 without being hydrolyzed since compound **6a** lacking the tosyl moiety is devoid of any activity or elicits weak effects. Interestingly, Nvb devoid of noviose was shown to lack the topoisomerase inhibitory capacity.<sup>32</sup> Then we can speculate that the lead analogues **6e** and **6f** would also be devoid of this activity. However, one could wonder if the noviose moiety linked to the 7-position of the coumarin ring is absolutely required for the biological activity of Nvb to inhibit hsp90 chaperoning function. Further work will probably help to understand such features.

## Conclusion

In this study, we have identified novobiocin analogues lacking the noviose moiety as a novel class of compounds related to hsp90 inhibition. The lead compounds **6e** and **6f** were the more potent in the four biological assays employed (e.g.: inhibitor of E<sub>2</sub>-induced and basal transactivation capacity of ER $\alpha$ , inducer of a proteasome-mediated degradation of ER $\alpha$ , HER2, Raf-1, and cdk4, inhibitor of cell cycle, and promoter of apoptosis and improved growth inhibition potential as compared to Nvb). In this regard, increasing evidence demonstrated that deregulation of the apoptotic signaling pathway is associated with tumorigenesis and resistance to many anticancer therapeutic agents thereby affecting patient outcome after chemotherapy.<sup>33</sup> Blagg et al.<sup>8b</sup> showed recently that the 4-hydroxyl and the 3'-carbamate are detrimental for hsp90 inhibitory activity. In this SAR study, we highlighted that in analogues lacking the noviose moiety, the introduction of a tosyl substituent on C-4 position of coumarin in **6e** contributed to a significant extent for maximal activity whereas analogue **6a** with a free 4-hydroxyl group was devoid of any activity. These initial findings have encouraged us to extensively explore novel 3-aminocoumarin analogues with different substituents at C-4 position and bearing or not a C-7 noviose moiety, to further investigate their biological activities and improve their potency as hsp90 inhibitors. The outcome of these studies will be reported in due course.

## Experimental Section

**Chemistry.** Melting points (mp) were recorded on a Büchi B-450 apparatus and were uncorrected. NMR spectra were performed on a Bruker AMX 200 (<sup>1</sup>H, 200 MHz; <sup>13</sup>C, 50 MHz), Bruker AVANCE 300, or Bruker AVANCE 400 (<sup>1</sup>H, 400 MHz; <sup>13</sup>C, 100 MHz). Unless otherwise stated, CDCl<sub>3</sub> was used as solvent. Chemical shifts  $\delta$  are in ppm, and the following abbreviations are used: singlet (s), doublet (d), triplet (t), multiplet (m), quintet (q), broad doublet (bd), broad multiplet (bm), broad triplet (bt), and broad singlet (bs). Elemental analyses (C, H, N) were performed at the Microanalyses Service of the Faculty of Pharmacy at Châtenay-Malabry (France) and were within 0.4% of the theoretical values otherwise stated. Mass spectra were obtained using a Bruker Esquire electrospray ionization apparatus.

**Materials.** DMF distilled from BaO, CH<sub>2</sub>Cl<sub>2</sub> distilled from calcium hydride, and the usual solvents were purchased from SDS (Paris, France). Liquid chromatography was performed on Merck silica gel 60 (70/30 mesh), and TLC was performed on silica gel, 60F-254 (0.26 mm thickness) plates. Visualization was achieved with UV light and phosphomolybdic acid reagent unless otherwise

stated. Monosodium novobiocin salt was purchased from Sigma-Aldrich, and geldanamycin and 17-AAG were provided by Kosan Laboratories. They were used at 200 and 2  $\mu$ M, respectively. Such concentrations were previously shown to have the maximal activity in various assays.<sup>9b</sup> The proteasome inhibitor MG132 was obtained from Sigma and used at 5  $\mu$ M. All other reagents were of high grade and used without further purification. The synthesized analogues **11**, **12**, **14**, and **15** were not biologically evaluated because they precipitate in cell culture medium at the concentrations used.

**N-(4,7-Dihydroxy-8-methyl-2-oxo-2H-chromen-3-yl)-4-hydroxy-3-(3-methylbut-2-enyl)benzamide (Novobiocic Acid 5a).**<sup>10</sup> Acetyl chloride (0.220 mL, 3.2 mmol) was added dropwise to a reflux solution of monosodium novobiocin salt (1.0 g, 1.6 mmol) in absolute ethanol (10 mL). A white precipitate appeared; the reaction mixture was stirred for 2 h at 78 °C and poured into ice/water (20 mL). The precipitate formed was collected, washed three times with frozen water, and dried under vacuum. Further purification by column chromatography on silica gel (cyclohexane/EtOAc: 6/4) gave 36% of **5a** (222.0 mg, 0.56 mmol) as a pale yellow solid. *R<sub>f</sub>* (cyclohexane/EtOAc: 6/4) 0.30; mp = 223–224 °C; <sup>1</sup>H NMR (400 MHz, DMSO-*d*<sub>6</sub>):  $\delta$  11.85 (s, 1H), 10.41 (s, 1H), 10.04 (s, 1H), 9.14 (s, 1H), 7.80 (s, 1H), 7.72 (d, *J* = 9.0 Hz, 1H), 7.54 (d, *J* = 8.8 Hz, 1H), 6.87 (d, *J* = 8.8 Hz, 1H), 6.85 (d, *J* = 9.0 Hz, 1H), 5.34 (t, *J* = 7.0 Hz, 1H), 2.15 (s, 3H), 2.06 (t, *J* = 7.0 Hz, 2H), 1.68 (s, 6H); <sup>13</sup>C NMR (100 MHz, DMSO-*d*<sub>6</sub>):  $\delta$  166.6, 160.9, 159.6, 159.0, 157.9, 151.3, 131.5, 129.8, 127.4, 127.3, 124.2, 122.6, 121.5, 114.3, 111.9, 110.5, 108.6, 100.5, 28.1, 25.6 (2C), 8.1; IR (cm<sup>-1</sup>): 3279, 2918, 1571, 1625, 1635, 1539, 1497, 1441, 1364, 1087, 817, 785, 760, 633; MS (ES<sup>+</sup>) *m/z* 418.2 ([M + Na]<sup>+</sup>, 100); Anal. (C<sub>22</sub>H<sub>21</sub>NO<sub>6</sub>) C, H, N.

**N-(4,7-Dimethoxy-8-methyl-2-oxo-2H-chromen-3-yl)-4-methoxy-3-(3-methylbut-2-enyl)benzamide (5b).** To a mixture containing **5a** (300.0 mg, 0.76 mmol, 1 equiv) and K<sub>2</sub>CO<sub>3</sub> (524 mg, 3.79 mmol, 20 equiv) in dry DMF (1 mL) and acetone (9 mL) was added dropwise dimethyl sulfate (360  $\mu$ L, 3.79 mmol, 20 equiv). After 24 h at room temperature, ethyl acetate (25 mL) was added and the organic layer washed with saturated aqueous NH<sub>4</sub>Cl (3  $\times$  25 mL), dried over Na<sub>2</sub>SO<sub>4</sub>, and concentrated under vacuum. Further purification by column chromatography on silica gel (cyclohexane/EtOAc: 6/4) gave 62% of **5b** (200 mg, 0.46 mmol) as a white solid. *R<sub>f</sub>* (CH<sub>2</sub>Cl<sub>2</sub>/MeOH: 9/1) 0.52; mp = 181–182 °C; <sup>1</sup>H NMR (400 MHz, CDCl<sub>3</sub>):  $\delta$  7.82 (dd, *J* = 8.4 and 2.4 Hz, 1H), 7.75 (d, *J* = 8.8 Hz, 1H), 7.74 (s, 1H), 7.61 (s, 1H), 6.91 (d, *J* = 8.8 Hz, 1H), 6.88 (d, *J* = 8.4 Hz, 1H), 5.33 (t, *J* = 7.2 Hz, 1H), 4.12 (s, 3H), 3.94 (s, 3H), 3.92 (s, 3H), 3.36 (d, *J* = 7.2 Hz, 2H), 2.31 (s, 3H), 1.77 (s, 3H), 1.74 (s, 3H); <sup>13</sup>C NMR (100 MHz, CDCl<sub>3</sub>):  $\delta$  167.0, 162.6, 160.6, 160.3, 159.7, 149.8, 133.8, 130.5, 129.1, 127.2, 125.2, 122.1, 121.5, 113.2, 111.2, 109.8, 107.0, 103.2, 59.3, 56.0, 55.5, 28.4, 25.5, 17.8, 8.2; IR (cm<sup>-1</sup>): 3311, 1695, 1672, 1601, 1489, 1454, 1247, 1117, 1023, 810, 758; MS (ES<sup>+</sup>) *m/z* 897.3 ([2M + Na]<sup>+</sup>, 100); Anal. (C<sub>25</sub>H<sub>27</sub>NO<sub>6</sub>) C, H, N.

**N-(4-Hydroxy-7-methoxy-8-methyl-2-oxo-2H-chromen-3-yl)-4-methoxy-3-(3-methylbut-2-enyl)benzamide (5c).** To a solution of **5b** (100 mg, 0.23 mmol, 1 equiv) in MeOH (4 mL) was added morpholine (402  $\mu$ L, 4.57 mmol, 20 equiv). The solution was heated under reflux for 5 h, a second portion of morpholine (402  $\mu$ L, 4.57 mmol, 20 equiv) was added, and the solution was heated under reflux overnight. After the mixture was cooled to room temperature, ethyl acetate was added and the organic layer was washed with an aqueous solution of 1 N HCl (pH = 1–2), dried over Na<sub>2</sub>SO<sub>4</sub>, filtered, and concentrated under vacuum. Further purification by column chromatography on silica gel (cyclohexane/EtOAc: 6/4) gave 65% of **5c** (63 mg, 0.15 mmol) as a white solid. *R<sub>f</sub>* (CH<sub>2</sub>Cl<sub>2</sub>/MeOH: 9/1) 0.67; mp = 207–210 °C; <sup>1</sup>H NMR (300 MHz, CDCl<sub>3</sub>):  $\delta$  14.05 (s, 1H), 8.73 (s, 1H), 7.82 (d, *J* = 8.8 Hz, 1H), 7.80 (dd, *J* = 8.4 and 2.4 Hz, 1H), 7.71 (d, *J* = 2.4 Hz, 1H), 6.91 (d, *J* = 8.8 Hz, 1H), 6.88 (d, *J* = 8.4 Hz, 1H), 5.31 (t, *J* = 7.2 Hz, 1H), 3.93 (s, 3H), 3.91 (s, 3H), 3.35 (d, *J* = 7.0 Hz, 2H), 2.30 (s, 3H), 1.77 (s, 3H), 1.74 (s, 3H); <sup>13</sup>C NMR (75 MHz, CDCl<sub>3</sub>):  $\delta$  166.9, 161.8, 161.3, 160.3, 153.4, 149.6, 133.8, 131.0, 128.7, 127.3,

123.4, 122.4, 121.3, 113.5, 110.5, 110.0, 107.3, 102.9, 56.0, 55.7, 28.3, 25.8, 17.8, 8.2; IR (cm<sup>-1</sup>): 3366, 1692, 1677, 1636, 1601, 1572, 1536, 1495, 1370, 1249, 1110, 1024, 809, 759, 630; MS (ES+) *m/z* 446 ([M + Na]<sup>+</sup>, 100); Anal. (C<sub>24</sub>H<sub>25</sub>NO<sub>6</sub>) C, H, N.

**2,2-Dimethylchroman-6-carboxylic Acid (4,7-dihydroxy-8-methyl-2-oxo-2H-chromen-3-yl)amide (Cyclonovobiocic Acid 6a).**<sup>10</sup> Aqueous chlorhydric acid (25 mL, 12 N) was added dropwise to a reflux solution of monosodium novobiocin salt (4.0 g, 6.3 mmol) in absolute ethanol (50 mL). A white precipitate appeared; the reaction mixture was stirred for 1 h at 78 °C. The solid formed was collected, washed three times with absolute ethanol, and dried under vacuum to give 99% of **6a** (2.47 g, 6.24 mmol) as a beige solid. *R<sub>f</sub>* (cyclohexane/EtOAc: 6/4) 0.46; mp = 286–287 °C; <sup>1</sup>H NMR (400 MHz, DMSO-*d*<sub>6</sub>): δ 11.80 (s, 1H), 10.40 (s, 1H), 9.20 (s, 1H), 7.80 (s, 1H), 7.73 (d, *J* = 8.6 Hz, 1H), 7.57 (d, *J* = 8.6 Hz, 1H), 6.88 (d, *J* = 8.6 Hz, 1H), 6.79 (d, *J* = 8.6 Hz, 1H), 2.88 (t, *J* = 6.6 Hz, 2H), 2.19 (s, 3H), 1.80 (t, *J* = 6.6 Hz, 2H), 1.30 (s, 6H); <sup>13</sup>C NMR (100 MHz, DMSO-*d*<sub>6</sub>): δ 161.8, 161.1, 160.0, 159.4, 157.0, 151.6, 130.4, 127.8, 125.1, 121.8, 120.8, 116.8, 112.2, 110.8, 108.4, 100.8, 75.4, 32.3, 26.8 (2C), 22.1, 8.4; IR (cm<sup>-1</sup>): 3191, 2977, 1660, 1627, 1602, 1567, 1538, 1366, 1096, 823; MS (TOF ES+) *m/z* 418 ([M + Na]<sup>+</sup>, 100); Anal. (C<sub>22</sub>H<sub>21</sub>NO<sub>6</sub>) C, H, N.

**2,2-Dimethylchroman-6-carboxylic Acid (4,7-Dimethoxy-8-methyl-2-oxo-2H-chromen-3-yl)amide (6b).** To a suspension of **6a** (600 mg, 1.52 mmol, 1 equiv) and K<sub>2</sub>CO<sub>3</sub> (4.19 g, 30.3 mmol, 1.1 equiv) in DMF (12 mL) was added dropwise dimethyl sulfate (2.88 mL, 30.3 mmol, 20 equiv). After the mixture was stirred 24 h at room temperature, ethyl acetate (40 mL) was added and the organic layer washed with saturated aqueous NH<sub>4</sub>Cl, dried over Na<sub>2</sub>SO<sub>4</sub>, and concentrated under vacuum. Further purification by column chromatography on silica gel (cyclohexane/EtOAc: 6/4) gave 61% of **6b** (393 mg, 0.93 mmol) as a white solid. *R<sub>f</sub>* (cyclohexane/EtOAc: 6/4) 0.35; mp = 237–238 °C; <sup>1</sup>H NMR (200 MHz, CDCl<sub>3</sub>): δ 8.24 (s, 1H), 7.70 (s, 1H), 7.63 (m, 2H), 6.82 (d, *J* = 8.9 Hz, 1H), 6.70 (d, *J* = 8.9 Hz, 1H), 4.12 (s, 3H), 3.89 (s, 3H), 2.73 (t, *J* = 6.6 Hz, 2H), 2.25 (s, 3H), 1.77 (t, *J* = 6.6 Hz, 2H), 1.33 (s, 6H); <sup>13</sup>C NMR (50 MHz, CDCl<sub>3</sub>): δ 167.0, 163.6, 160.7, 160.3, 157.5, 152.0, 129.5, 127.1, 124.0, 122.0, 120.8, 117.1, 113.3, 111.0, 106.9, 102.9, 75.1, 59.3, 55.8, 32.4, 26.8 (2C), 22.2, 8.0; IR (cm<sup>-1</sup>): 3282, 1715, 1604, 1500, 1479, 1354, 1153, 881, 763; MS (ES+) *m/z* 446.3 ([M + Na]<sup>+</sup>, 100); Anal. (C<sub>24</sub>H<sub>25</sub>NO<sub>6</sub>) C, H, N.

**2,2-Dimethylchroman-6-carboxylic Acid (7-Hydroxy-4-methoxy-8-methyl-2-oxo-2H-chromen-3-yl)amide (6c).** To a suspension of **6a** (200 mg, 0.51 mmol, 1 equiv) and K<sub>2</sub>CO<sub>3</sub> (77 mg, 0.55 mmol, 1.1 equiv) in DMF (5 mL) was added dropwise dimethyl sulfate (55 μL, 0.55 mmol, 1.1 equiv). After the mixture was stirred 48 h at room temperature, ethyl acetate was added to the solution. The organic layer was washed with a saturated aqueous solution of NH<sub>4</sub>Cl, dried over Na<sub>2</sub>SO<sub>4</sub>, filtered, and concentrated under vacuum. Further purification by column chromatography on silica gel (cyclohexane/EtOAc: 6/4) gave 20% of **6c** (38 mg, 93 μmol) as a white solid. *R<sub>f</sub>* (cyclohexane/EtOAc: 6/4) 0.17; mp = 223–224 °C; <sup>1</sup>H NMR (400 MHz, DMSO-*d*<sub>6</sub>): δ 10.50 (s, 1H), 9.41 (s, 1H), 7.76 (s, 1H), 7.70 (d, *J* = 8.6 Hz, 1H), 7.50 (d, *J* = 8.8 Hz, 1H), 6.86 (d, *J* = 8.8 Hz, 1H), 6.79 (d, *J* = 8.6 Hz, 1H), 4.07 (s, 3H), 2.79 (t, *J* = 6.6 Hz, 2H), 2.14 (s, 3H), 1.79 (t, *J* = 6.6 Hz, 2H), 1.29 (s, 6H); <sup>13</sup>C NMR (100 MHz, DMSO-*d*<sub>6</sub>): δ 166.5, 161.5, 161.3, 159.1, 156.8, 150.6, 129.8, 127.1, 124.7, 121.5, 120.7, 116.6, 112.0, 110.4, 108.4, 102.4, 75.1, 59.8, 31.8, 26.5 (2C), 21.7, 8.0; IR (cm<sup>-1</sup>): 3284, 2935, 1673, 1595, 1570, 1537, 1491, 1366, 1254, 1114, 947, 759, 746; MS (ES+) *m/z* 432 ([M + Na]<sup>+</sup>, 25), 242.0 (100); Anal. Calcd for C<sub>23</sub>H<sub>23</sub>NO<sub>6</sub>: C, 67.47; H, 5.66; N, 3.42. Found: C, 66.61; H, 5.75; N, 3.35.

**2,2-Dimethylchroman-6-carboxylic Acid (4-Hydroxy-7-methoxy-8-methyl-2-oxo-2H-chromen-3-yl)amide (6d).** To a solution of **6b** (100 mg, 0.24 mmol, 1 equiv) in MeOH (4 mL) was added morpholine (414 μL, 4.72 mmol, 20 equiv). The solution was heated under reflux for 16 h, a second portion of morpholine (414 μL, 4.72 mmol, 20 equiv) was added, and the solution was heated under reflux for 48 h. After the mixture was cooled to room temperature,

ethyl acetate was added and the organic layer washed with an aqueous solution of 1 N HCl (pH = 1–2), dried over Na<sub>2</sub>SO<sub>4</sub>, filtered, and concentrated under vacuum. Further purification by column chromatography on silica gel (cyclohexane/EtOAc: 6/4) gave 98% of **6d** (95 mg, 0.23 mmol) as a white solid. *R<sub>f</sub>* (cyclohexane/EtOAc: 6/4) 0.67; mp = 207–209 °C; <sup>1</sup>H NMR (400 MHz, CDCl<sub>3</sub>): δ 14.07 (s, 1H), 8.71 (s, 1H), 7.85 (d, *J* = 8.8 Hz, 1H), 7.70 (m, 2H), 6.89 (m, 2H), 3.93 (s, 3H), 2.87 (t, *J* = 6.6 Hz, 2H), 2.32 (s, 3H), 1.86 (t, *J* = 6.6 Hz, 2H), 1.38 (s, 6H); <sup>13</sup>C NMR (100 MHz, CDCl<sub>3</sub>): δ 166.9, 161.8, 160.3, 158.6, 153.5, 148.2, 129.6, 127.1, 122.6, 122.4, 121.5, 117.9, 113.5, 110.6, 107.4, 102.9, 75.7, 56.0, 32.4, 26.9 (2C), 22.4, 8.0; IR (cm<sup>-1</sup>): 3286, 1673, 1596, 1493, 1367, 1255, 1115, 803; MS (ES-) *m/z* 408.0 ([M - H]<sup>-</sup>, 100); Anal. Calcd for C<sub>23</sub>H<sub>23</sub>NO<sub>6</sub>: C, 67.47; H, 5.66; N, 3.42. Found: C, 66.71; H, 5.83; N, 3.40.

**Toluene-4-sulfonic Acid 3-[(2,2-Dimethylchroman-6-carboxyl)amino]-7-hydroxy-8-methyl-2-oxo-2H-chromen-4-yl Ester (6e).** A solution of *p*TsCl (530 mg, 2.78 mmol, 1.1 equiv) in pyridine (5 mL) was added slowly to an ice-cooled suspension of **6a** (1.0 g, 2.53 mmol, 1 equiv) in dry pyridine (10 mL). After the mixture was stirred 24 h at room temperature, ethyl acetate (25 mL) was added and the organic layer washed with aqueous 1 N HCl (pH = 1–2), dried over Na<sub>2</sub>SO<sub>4</sub>, and concentrated under vacuum. Further purification by column chromatography on silica gel (cyclohexane/EtOAc: 6/4) gave 53% of **6e** (743 mg, 1.35 mmol) as a white solid. *R<sub>f</sub>* (cyclohexane/EtOAc: 6/4) 0.20; mp = 163–165 °C; <sup>1</sup>H NMR (400 MHz, CDCl<sub>3</sub>): δ 8.50 (s, 1H), 7.74 (d, *J* = 8.3 Hz, 2H), 7.68 (s, H+NH), 7.59 (d, *J* = 8.5 Hz, 1H), 7.24 (d, *J* = 8.3 Hz, 2H), 6.85 (d, *J* = 8.5 Hz, 1H), 6.53 (d, *J* = 8.7 Hz, 1H), 6.49 (d, *J* = 8.7 Hz, 1H), 2.86 (t, *J* = 6.5 Hz, 2H), 2.40 (s, 3H), 2.13 (s, 3H), 1.88 (t, *J* = 6.5 Hz, 2H), 1.40 (s, 6H); <sup>13</sup>C NMR (100 MHz, CDCl<sub>3</sub>): δ 167.2, 160.2, 159.5, 158.4, 152.2, 150.9, 146.5, 132.5, 130.2 (2C), 128.1 (3C), 127.3, 123.3, 121.4, 121.2, 117.5, 112.8, 112.5, 111.9, 108.1, 75.6, 32.5, 26.9 (2C), 22.4, 21.8, 8.0; IR (cm<sup>-1</sup>): 3250, 3100, 1696, 1592, 1363, 1256, 810, 761, 733, 656; MS (ES-) *m/z* 548.3 ([M - H]<sup>-</sup>, 100), 1097.2 ([2M - H]<sup>-</sup>, 16); Anal. (C<sub>29</sub>H<sub>27</sub>NO<sub>8</sub>S) C, H, N.

**Toluene-4-sulfonic Acid 3-[(2,2-Dimethylchroman-6-carboxyl)amino]-4-hydroxy-8-methyl-2-oxo-2H-chromen-7-yl Ester (6f).** A solution of *p*TsCl (530 mg, 2.78 mmol, 1.1 equiv) in dry THF (3 mL) was added slowly to an ice-cooled suspension of **6a** (1.0 g, 2.53 mmol, 1 equiv) and DMAP (309 mg, 2.53 mmol, 1 equiv) in a mixture of dry THF (30 mL) and TEA (5 mL). After the mixture was stirred for 48 h at room temperature, ethyl acetate (50 mL) was added and the organic layer washed with aqueous 1 N HCl, dried over Na<sub>2</sub>SO<sub>4</sub>, and concentrated under vacuum. Further purification by column chromatography on silica gel (CH<sub>2</sub>Cl<sub>2</sub>) gave 54% of **6f** (736 mg, 1.34 mmol) as a white solid. *R<sub>f</sub>* (cyclohexane/EtOAc: 6/4) 0.59; mp = 197–198 °C; <sup>1</sup>H NMR (400 MHz, CDCl<sub>3</sub>): δ 14.16 (s, 1H), 8.70 (s, 1H), 7.74 (m, 5H), 7.35 (d, *J* = 8.0 Hz, 2H), 7.10 (d, *J* = 8.6 Hz, 1H), 6.88 (d, *J* = 8.6 Hz, 1H), 2.87 (t, *J* = 6.7 Hz, 2H), 2.47 (s, 3H), 2.16 (s, 3H), 1.86 (t, *J* = 6.7 Hz, 2H), 1.38 (s, 6H); <sup>13</sup>C NMR (100 MHz, CDCl<sub>3</sub>): δ 167.3, 161.1, 159.0, 152.2, 150.1, 149.3, 145.9, 132.8, 130.0 (2C), 129.8, 128.5 (2C), 127.2, 122.2, 121.6 (2C), 120.3, 118.9, 118.0, 116.0, 104.8, 75.8, 32.4, 26.9 (2C), 22.4, 21.8, 9.5; IR (cm<sup>-1</sup>): 3360, 3100, 1697, 1596, 1536, 1489, 1484, 1374, 1074, 847, 811, 766, 733, 644, 616; MS (ES-) *m/z* 548 ([M - H]<sup>-</sup>, 100); Anal. (C<sub>29</sub>H<sub>27</sub>NO<sub>8</sub>S) C, H, N.

**Toluene-4-sulfonic Acid 4-(4-Chlorophenyl)-3-[(2,2-dimethylchroman-6-carboxyl)amino]-8-methyl-2-oxo-2H-chromen-7-yl Ester (6h).** A solution **6e** (50 mg, 91 μmol, 1 equiv), 4-chlorophenylboronic acid (18 mg, 0.12 mmol, 1.3 equiv), K<sub>3</sub>PO<sub>4</sub> (58 mg, 0.27 mmol, 3 equiv), Bu<sub>4</sub>NBr (3 mg, 9.1 μmol, 10 mol %), and PdCl<sub>2</sub>(dppf) (4 mg, 4.5 μmol, 5 mol %) in CH<sub>3</sub>CN was heated at 80 °C for 3 h. After the mixture was cooled to room temperature, ethyl acetate was added. The organic layer was washed with water, dried over Na<sub>2</sub>SO<sub>4</sub>, and concentrated under vacuum. Further purification by column chromatography on silica gel (cyclohexane/EtOAc: 6/4) gave 41% of **6h** (24 mg, 37.0 μmol) as a white solid. *R<sub>f</sub>* (cyclohexane/EtOAc: 6/4) 0.35; mp = 117–120



$^{\circ}\text{C}$ ;  $^1\text{H}$  NMR (400 MHz,  $\text{CDCl}_3$ ):  $\delta$  7.75 (d,  $J$  = 8.2 Hz, 2H), 7.58 (s, 1H), 7.46 (s, 1H), 7.42 (d,  $J$  = 8.3 Hz, 2H), 7.41 (dd,  $J$  = 8.4 and 1.9 Hz, 1H), 7.37 (d,  $J$  = 8.2 Hz, 2H), 7.36 (d,  $J$  = 8.2 Hz, 2H), 7.10 (d,  $J$  = 8.9 Hz, 1H), 7.06 (d,  $J$  = 8.9 Hz, 1H), 6.75 (d,  $J$  = 8.4 Hz, 1H), 2.76 (t,  $J$  = 6.8 Hz, 2H), 2.49 (s, 3H), 2.13 (s, 3H), 1.81 (t,  $J$  = 6.8 Hz, 2H), 1.44 (s, 6H);  $^{13}\text{C}$  NMR (100 MHz,  $\text{CDCl}_3$ ):  $\delta$  165.2, 159.6, 158.0, 150.6, 150.0, 149.5, 145.9, 144.5, 134.8, 132.5, 131.5, 130.0 (4C), 129.5, 129.0 (2C), 128.2 (2C), 126.5, 124.5, 124.2, 121.1, 120.2, 118.9, 118.2, 117.2, 75.2, 33.0, 27.0 (2C), 22.1, 21.9, 9.0; IR ( $\text{cm}^{-1}$ ): 2939, 1739, 1575, 1498, 1232, 830; MS (ES+)  $m/z$  644.2 ( $[\text{M}]^+$ , 16), 661.1 ( $[\text{M} + \text{Na}]^+$ , 100), 668.1 (18), 703.2 (16); Anal. Calcd for  $(\text{C}_{35}\text{H}_{30}\text{ClNO}_7\text{S} \cdot 3.0\text{H}_2\text{O})$ : C, 60.21; H, 5.20; N, 2.01. Found: C, 59.61; H, 4.45; N, 1.84.

**Toluene-4-sulfonic Acid 3-[(2,2-Dimethylchroman-6-carboxyl)amino]-7-methoxy-8-methyl-2-oxo-2H-chromen-4-yl Ester (6i).** A solution of *p*TsCl (458 mg, 2.40 mmol, 2.0 equiv) in pyridine (3 mL) was added slowly to an ice-cooled suspension of **6d** (493 mg, 1.20 mmol, 1 equiv) in dry pyridine (3 mL). After the mixture was stirred 24 h at room temperature, ethyl acetate (25 mL) was added, the organic layer washed with aqueous 1 N HCl (pH = 1–2), dried over  $\text{Na}_2\text{SO}_4$ , and concentrated under vacuum. Further purification by column chromatography on silica gel (cyclohexane/EtOAc: 7/3) gave 57% of **6i** (385 mg, 0.68 mmol) as a white solid.  $R_f$  (cyclohexane/EtOAc: 7/3) 0.20; mp = 184–185  $^{\circ}\text{C}$ ;  $^1\text{H}$  NMR (300 MHz,  $\text{CDCl}_3$ ):  $\delta$  7.78 (d,  $J$  = 8.1 Hz, 2H), 7.54 (d,  $J$  = 8.7 Hz, 1H), 7.50 (d,  $J$  = 2.1 Hz, 1H), 7.43 (bs, 1H), 7.38 (dd,  $J$  = 8.7 and 2.1 Hz, 1H), 7.14 (d,  $J$  = 8.1 Hz, 2H), 6.87 (d,  $J$  = 8.7 Hz, 1H), 6.77 (d,  $J$  = 8.7 Hz, 1H), 3.93 (s, 3H), 2.82 (t,  $J$  = 6.6 Hz, 2H), 2.30 (s, 6H), 1.85 (t,  $J$  = 6.6 Hz, 2H), 1.37 (s, 6H);  $^{13}\text{C}$  NMR (75 MHz,  $\text{CDCl}_3$ ):  $\delta$  164.2, 160.9, 160.7, 157.8, 149.8, 149.0, 145.8, 133.4, 129.9 (2C), 129.8, 128.0 (2C), 127.0, 124.0, 122.6, 120.8, 117.1, 114.1, 113.2, 110.7, 107.6, 75.3, 56.1, 32.5, 26.9 (2C), 22.3, 21.6, 8.2; IR ( $\text{cm}^{-1}$ ): 3313, 1703, 1605, 1579, 1360, 1293, 1118; MS (ES+)  $m/z$  431 ( $[\text{M} - \text{OTs} + \text{K}]^+$ , 16), 564 ( $[\text{M} + \text{H}]^+$ , 18), 586 ( $[\text{M} + \text{Na}]^+$ , 100); Anal. ( $\text{C}_{30}\text{H}_{29}\text{NO}_8\text{S}$ ) C, H, N.

**2,2-Dimethylchroman-6-carboxylic Acid [7-Methoxy-4-(4-methoxyphenyl)-8-methyl-2-oxo-2H-chromen-3-yl]amide (6j).** A solution of **6i** (100 mg, 0.18 mmol, 1 equiv), 4-methoxyphenylboronic acid (35 mg, 0.23 mmol, 1.3 equiv),  $\text{K}_3\text{PO}_4$  (116 mg, 0.54 mmol, 3 equiv),  $\text{Bu}_4\text{NBr}$  (6 mg, 18.2  $\mu\text{mol}$ , 10 mol %), and  $\text{PdCl}_2(\text{dppf})$  (8 mg, 9  $\mu\text{mol}$ , 5 mol %) in  $\text{CH}_3\text{CN}$  (2 mL) was heated at 80  $^{\circ}\text{C}$  for 3 h. After the mixture was cooled to room temperature, ethyl acetate was added. The organic layer was washed with water, dried over  $\text{Na}_2\text{SO}_4$ , and concentrated under vacuum. Further purification by column chromatography on silica gel (cyclohexane/EtOAc: 6/4) gave 92% of **6j** (83 mg, 0.17 mmol) as a white solid.  $R_f$  (cyclohexane/EtOAc: 6/4) 0.19; mp = 225–226  $^{\circ}\text{C}$ ;  $^1\text{H}$  NMR (300 MHz,  $\text{CDCl}_3$ ):  $\delta$  7.47 (bs, 2H), 7.39 (dd,  $J$  = 8.5 and 2.1 Hz, 1H), 7.34 (d,  $J$  = 8.7 Hz, 2H), 7.12 (d,  $J$  = 8.5 Hz, 1H), 6.95 (d,  $J$  = 8.7 Hz, 2H), 6.74 (d,  $J$  = 9.0 Hz, 1H), 6.69 (d,  $J$  = 9.0 Hz, 1H), 3.89 (s, 3H), 3.80 (s, 3H), 2.71 (t,  $J$  = 6.5 Hz, 2H), 2.33 (s, 3H), 1.77 (t,  $J$  = 6.5 Hz, 2H), 1.31 (s, 6H);  $^{13}\text{C}$  NMR (75 MHz,  $\text{CDCl}_3$ ):  $\delta$  165.9, 159.9, 159.7, 157.4, 151.2, 148.5, 129.9 (2C), 129.6, 126.6, 125.7, 125.5, 124.9, 120.8 (2C), 117.7, 117.1, 114.2, 114.0, 113.9 (2C), 107.0, 75.2, 56.0, 55.2, 32.4, 26.8 (2C), 22.2, 8.2; IR ( $\text{cm}^{-1}$ ): 2973, 1737, 1636, 1600, 1511, 1481, 1266, 1249, 1117, 847, 764; MS (ES+)  $m/z$  500 ( $[\text{M} + \text{H}]^+$ , 11), 522 ( $[\text{M} + \text{Na}]^+$ , 100), 538 ( $[\text{M} + \text{K}]^+$ , 16); Anal. ( $\text{C}_{30}\text{H}_{29}\text{NO}_6$ ) C, H, N.

**Biology. Cell Culture and Drug Treatment.** MCF-7 and MELN cells (MCF-7 cells established after stable transfection with a construct in which the LUC reporter gene is placed under the control of an estrogen responsive element (ERE) linked to the minimal  $\beta$ -globin promoter (ERE- $\beta$ -globin-LUC)<sup>34</sup>) were grown in Dulbecco's modified eagle medium (DMEM) in the presence of 10% fetal calf serum (FCS). For transcription measurements in MELN cells, the culture medium was replaced by phenol red free DMEM containing 10% stripped serum (charcoal Norit A 1%, Dextran 0.1%, 30 min at room temperature) at least 2 days before cell exposure to steroids or other drugs. Cells were incubated with GA (2  $\mu\text{M}$ ), Nvb, and analogues (200  $\mu\text{M}$ ) in the presence or not of 0.1 nM  $\text{E}_2$ , a concentration previously determined as giving the

maximum of induced LUC activity.<sup>20</sup> After 18 h exposure, cells were collected, rinsed, and lysed in 250  $\mu\text{L}$  of the LUC buffer (Tris 25 mM,  $\text{MgCl}_2$  10 mM, Triton X100 1%, glycerol 15%, EDTA 1 mM, DTT 1 mM,  $\text{H}_3\text{PO}_4$  pH = 7.8). Protein concentration was determined by the Biorad Assay (Bio Rad GmbH, Munich, Germany). Quantification of the LUC activity was performed in a luminometer (Lumat LB 9507, Berthold-France, Thoiry, France), after injection of the LUC buffer (100  $\mu\text{L}$ ) supplemented with 100 mM ATP and 87  $\mu\text{g}$  luciferine/mL, to 100  $\mu\text{L}$  of cellular extract.

**Quantification of Cell Survival/Proliferation.** Cells were seeded in 96-well plates at 5000 cells/well, and after 24 h, serial dilutions of drugs were added. After 72 h, 3-(4,5-dimethylthiazol-2-yl)-2,5-diphenyltetrazolium bromide (MTT, Sigma) (500  $\mu\text{g}/\text{mL}$ ) was added to each well during 3 h at 37  $^{\circ}\text{C}$ . Medium was removed and MTT formazan crystals were dissolved in 100  $\mu\text{L}$  of DMSO followed by gentle agitation for 10 min. The absorbance of converted dye which directly correlates with the number of viable cells was measured at 570 nm with background subtraction at 650 nm using a spectrophotometric microtiter reader (Metertech,  $\Sigma$ 960, Fisher-Bioblock, Illkirch, France). All determinations were carried out in sextuplicate, and each experiment was repeated three times. The percentage of survival was calculated as the absorbance ratio of treated to untreated cells. The  $\text{IC}_{50}$  values were determined as the drug concentrations that inhibit cell growth by 50% compared with growth of vehicle-treated cells.

**Cell Extracts and Western Blots.** Cells were grown to 50% confluence in 60-mm dishes before exposure to various agents as indicated in the text and figure legends. Cells were rinsed in PBS, scraped into PBS, collected by centrifugation, and resuspended in ice-cold lysis buffer (Tris-HCl 50 mM (pH 7.5), NaCl 150 mM, EGTA 1 mM, glycerol 10% (v/v), Triton X-100 1%,  $\text{MgCl}_2$  1.5 mM, NaF 10 mM, Na pyrophosphate 10 mM,  $\text{Na}_3\text{VO}_4$  1 mM) plus protease inhibitors (Complete reagent, Roche Diagnostics, Indianapolis, IN) and kept on ice for 15 min with occasional vortexing. Insoluble debris were removed by centrifugation at 15 000g for 5 min at 4  $^{\circ}\text{C}$ , and cell lysates were boiled in Laemmli sample buffer for 3 min. TCEs were obtained from pelleted cells by resuspension in lysis buffer for 30 min at 4  $^{\circ}\text{C}$  and boiling for 5 min in Laemmli sample buffer. Protein concentration was determined by the Bio-Rad Assay. Equal amounts of protein (20  $\mu\text{g}$ ) were fractionated by 8% or 12% SDS-polyacrylamide gel electrophoresis (SDS-PAGE) and transferred onto Immobilon-P membranes (Millipore, Saint Quentin en Yvelines, France). Membranes were blocked for 1 h at 37  $^{\circ}\text{C}$  with 10% dry nonfat milk in PBS containing 0.1% Tween 20. ER $\alpha$  was detected with the D12 (ER epitope: amino acids 2–185) (Santa Cruz, CA) mouse monoclonal anti-ER antibody used at 1  $\mu\text{g}/\text{mL}$  in PBST–2% milk overnight at 4  $^{\circ}\text{C}$ . The antigen/antibody complexes were detected by incubation with a biotinylated anti-mouse antibody followed by revelation with the avidin–peroxidase complex (Vectastain ABC Elite Kit, Vector Laboratories, Inc., Burlingame, CA). Other primary antibodies were: HER2 (C18), Raf-1 (C12), cdk4 (C22), caspase 7 (B5), and PARP (F-2) from Santa Cruz and caspase 8 (1C12) from Cell Signaling (Beverly, MA) used at 1  $\mu\text{g}/\text{mL}$ . The antigen/antibody complexes were detected with appropriate secondary horseradish peroxidase-conjugated antibodies (Santa Cruz). Blots were developed using the Immobilon Western Detection Reagent (Millipore). Depending on the mobility of the proteins, membranes were either stripped (1 h at 50  $^{\circ}\text{C}$  in a medium containing 62.5 mM Tris-HCl pH 6.8, 2% SDS, and 100 mM 2-mercaptoethanol) or extensively washed before reprobing with different primary antibodies. Equal protein loading was assessed by examination of the intensities of nonspecific (NS) signals elicited by the commercial antibodies used and unresponsive to treatments.

**Flow Cytometry Analysis.** Cells ( $1.3 \times 10^5$  cells/mL) were cultured in the presence or not of novobiocin analogues at 200  $\mu\text{M}$ . Nvb at the same concentration served as reference inhibitor. After treatment for 48 and 72 h, cells were washed and fixed in PBS/ethanol (30/70). For cytofluorometric examination, cells ( $10^4$ ) were incubated for 30 min in PBS/ Triton X100, 0.2% EDTA 1 mM, and propidium iodide (PI) (50  $\mu\text{g}/\text{mL}$ ) in PBS supplemented by

RNase (0.5 mg/mL). The number of cells in the different phases of the cell cycle was determined, and the percentage of apoptotic cells was quantified. Analyses were performed with a FACS Calibur (Becton Dickinson, Le Pont de Claix, France). Cell Quest software was used for data acquisition and analysis.

**Acknowledgment.** We thank the Ligue Nationale contre le Cancer (Cher and Indre Committees, grants to J.-M.R.), the Minister dell'Istruzione dell'Università e della Ricerca (MIUR, fellowship to B.S.), and the Société de Chimie Thérapeutique (SERVIER group) for the fellowship to G.L.B. We also thank M. G. Catelli for criticism and support during this work.

**Supporting Information Available:** Experimental procedures and spectral data for compounds 11–16. This material is available free of charge via the Internet at <http://pubs.acs.org>.

## References

- (a) Pratt, W. B.; Toft, D. O. Regulation of signaling protein function and trafficking by the hsp90/hsp70-based chaperone machinery. *Exp. Biol. Med. (Maywood, NJ, U.S.A.)* **2003**, *228*, 111–133. (b) Isaacs, J. S.; Xu, W.; Neckers, L. Heat shock protein 90 as a molecular target for cancer therapeutics. *Cancer Cell* **2003**, *3*, 213–217.
- (a) Richter, K.; Buchner, J. Hsp90: Chaperoning signal transduction. *J. Cell. Physiol.* **2001**, *188*, 281–290. (b) Neckers, L. Hsp90 inhibitors as novel cancer chemotherapeutic agents. *Trends Mol. Med.* **2002**, *8*, S55–S61. (c) Neckers, L.; Ivy, S. P. Heat shock protein 90. *Curr. Opin. Oncol.* **2003**, *15*, 419–424. (d) Zhang, H.; Burrows, F. Targeting multiple signal transduction pathways through inhibition of Hsp90. *J. Mol. Med.* **2004**, *82*, 488–499.
- (a) Hanahan, D.; Weinberg, R. A. The hallmarks of cancer. *Cell* **2000**, *100*, 57–70.
- (a) Janin, Y. L. Heat shock protein 90 inhibitors: a text book example of medicinal chemistry? *J. Med. Chem.* **2005**, *48*, 7503–7512. (b) Chiosis, G.; Rodina, A.; Moulick, K. Emerging Hsp90 inhibitors: From discovery to clinic. *Anticancer Agents Med. Chem.* **2006**, *6*, 1–8. (c) He, H.; Zatorska, D.; Kim, J.; Aguirre, J.; Llauger, L.; She, Y.; Wu, N.; Immormino, R. M.; Gewirth, D. T.; Chiosis, G. Identification of potent water soluble purine-scaffold inhibitors of the heat shock protein 90. *J. Med. Chem.* **2006**, *49*, 381–390.
- (a) Marcu, M. G.; Chadli, A.; Bouhouche, I.; Catelli, M.; Neckers, L. M. The heat shock protein 90 antagonist novobiocin interacts with a previously unrecognized ATP-binding domain in the carboxyl terminus of the chaperone. *J. Biol. Chem.* **2000**, *275*, 37181–37186.
- (a) Marcu, M. G.; Schulte, T. W.; Neckers, L. Novobiocin and related coumarins and depletion of heat shock protein 90-dependent signaling proteins. *J. Natl. Cancer Inst.* **2000**, *92*, 242–248.
- (a) Roe, S. M.; Prodromou, C.; O'Brien, R.; Ladbury, J. E.; Piper, P. W.; Pearl, L. H. Structural basis for inhibition of the Hsp90 molecular chaperone by the antitumor antibiotics radicicol and geldanamycin. *J. Med. Chem.* **1999**, *42*, 260–266. (b) Schulte, T. W.; Akinaga, S.; Murakata, T.; Agatsuma, T.; Sugimoto, S.; Nakano, H.; Lee, Y. S.; Simen, B. B.; Argon, Y.; Felts, S.; Toft, D. O.; Neckers, L. M.; Sharma, S. V. Interaction of radicicol with members of the heat shock protein 90 family of molecular chaperones. *Mol. Endocrinol.* **1999**, *13*, 1435–1448. (c) Blagosklonny, M. V. Hsp90-associated oncoproteins: multiple targets of geldanamycin and its analogs. *Leukemia* **2002**, *16*, 455–462.
- (a) Yu, X. M.; Shen, G.; Neckers, L.; Blake, H.; Holzbeierlein, J.; Cronk, B.; Blagg, B. S. J. Hsp90 inhibitors identified from a library of novobiocin analogues. *J. Am. Chem. Soc.* **2005**, *127*, 12778–12779. (b) Burlison, J. A.; Neckers, L.; Smith, A. B.; Maxwell, A.; Blagg, B. S. J. Novobiocin: redesigning a DNA gyrase inhibitor for selective inhibition of Hsp90. *J. Am. Chem. Soc.* **2006**, *128*, 15529–15536.
- (a) Galigiana, M. D.; Radanyi, C.; Renoir, J. M.; Housley, P. R.; Pratt, W. B. Evidence that the peptidylprolyl isomerase domain of the hsp90-binding immunophilin FKBP52 is involved in both dynein interaction and glucocorticoid receptor movement to the nucleus. *J. Biol. Chem.* **2001**, *276*, 14884–14889. (b) Gougelet, A.; Bouclier, C.; Marsaud, V.; Maillard, S.; Mueller, S. O.; Korach, K. S.; Renoir, J. M. Estrogen receptor alpha and beta subtype expression and transactivation capacity are differentially affected by receptor-, hsp90- and immunophilin-ligands in human breast cancer cells. *J. Steroid Biochem. Mol. Biol.* **2005**, *94*, 71–81.
- (a) Hinman, J. W.; Caron, E. L.; Hoeksema, H. The structure of novobiocin. *J. Am. Chem. Soc.* **1957**, *79*, 3789–3800. (b) Spencer, C. F.; Rodin, J. O.; Walton, E.; Holly, F. W.; Folkers, K. Novobiocin. VII. Synthesis of novobiocic acid, dihydronovobiocic acid and cyclonovobiocic acid. *J. Am. Chem. Soc.* **1958**, *80*, 140–143.
- (a) Wu, J.; Wang, L.; Fathi, R.; Yang, Z. Palladium-catalyzed cross-coupling reactions of 4-tosylcoumarin and arylboronic acids: synthesis of 4-arylcoumarin compounds. *Tetrahedron Lett.* **2002**, *43*, 4395–4397. (b) Boland, G. M.; Donnelly, D. M. X.; Finet, J. P.; Rea, M. D. Synthesis of neoflavones by Suzuki arylation of 4-substituted coumarins. *J. Chem. Soc., Perkin Trans. 1* **1996**, 2591–2597.
- (a) Fringuelli, F.; Piermatti, O.; Pizzo, F. One-pot synthesis of 3-carboxycoumarins via consecutive Knoevenagel and Pinner reactions in water. *Synthesis* **2003**, 2331–2334. (b) Bonsignore, L.; Cottiglia, F.; Maccioni, A. M.; Secci, D.; Lavagna, S. M. Synthesis of coumarin-3-O-acylisoureas by dicyclohexylcarbodiimide. *J. Heterocycl. Chem.* **1995**, *32*, 573–577.
- Bansal, V.; Kanodia, S.; Thapliyal, P. C.; Khanna, R. N. Microwave induced selective bromination of 1,4-quinones and coumarins. *Synth. Commun.* **1996**, *26*, 887–892.
- (a) Schiedel, M. S.; Briehn, C. A.; Bäuerle, P. C-C cross-coupling reactions for the combinatorial synthesis of novel organic materials. *J. Organomet. Chem.* **2002**, *653*, 200–208. (b) Schiedel, M. S.; Briehn, C. A.; Bäuerle, P. Single compound libraries of organic materials: Parallel synthesis and screening of fluorescent dyes. *Angew. Chem., Int. Ed. Engl.* **2001**, *40*, 4677–4680.
- (a) Olivi, N.; Thomas, E.; Peyrat, J.-F.; Alami, M.; Brion, J.-D. Highly efficient *p*-toluenesulfonic acid-catalyzed alcohol addition or hydration of unsymmetrical arylalkynes. *Synlett* **2004**, 2175–2179. (b) Le, Bras, G.; Provot, O.; Peyrat, J.-F.; Alami, M.; Brion, J.-D. Rapid microwave assisted hydration of internal arylalkynes in the presence of PTSA: an efficient regioselective access to carbonyl compounds. *Tetrahedron Lett.* **2006**, *47*, 5497–5501.
- (a) Hostein, I.; Robertson, D.; DiStefano, F.; Workman, P.; Clarke, P. A. Inhibition of signal transduction by the hsp90 inhibitor 17-Allylamino-17-demethoxygeldanamycin results in cytostasis and apoptosis. *Cancer Res.* **2001**, *61*, 4003–4009. (b) Münster, P. N.; Basso, A.; Solit, D.; Norton, L.; Rosen, N. Modulation of hsp90 function by ansamycins sensitizes breast cancer cells to chemotherapy-induced apoptosis in an RB- and schedule-dependent manner. *Clin. Cancer Res.* **2001**, *7*, 2228–2236. (c) Solit, D. B.; Zheng, F. F.; Drobnjak, M.; Münster, P. N.; Higgins, B.; Verbel, D.; Heller, G.; Tong, W.; Cordon-Cardo, C.; Agus, D. B.; Scher, H. I.; Rosen, N. 17-Allylamino-17-demethoxygeldanamycin induces the degradation of androgen receptor and HER-2/*neu* and inhibits the growth of prostate cancer xenografts. *Clin. Cancer Res.* **2002**, *8*, 986–993. (d) Rodina, A.; Vilenchik, M.; Moulick, K.; Aguirre, J.; Kim, J.; Chiang, A.; Litz, J.; Clement, C. C.; Kang, Y.; She, Y.; Wu, N.; Felts, S.; Wipf, P.; Massague, J.; Jiang, X.; Brodsky, J. L.; Krystal, G. W.; Chiosis, G. Selective compounds define Hsp90 as a major inhibitor of apoptosis in small-cell lung cancer. *Nat. Chem. Biol.* **2007**, *3*, 498–507.
- (a) Burrows, F.; Zhang, H.; Kamal, A. Hsp90 activation and cell cycle regulation. *Cell Cycle* **2004**, *12*, 1530–1536. (b) Pearl, L. H.; Prodromou, C. Structure and mechanism of the hsp90 molecular chaperone machinery. *Annu. Rev. Biochem.* **2006**, *75*, 271–294.
- (a) Stebbins, C. E.; Russo, A. A.; Schneider, C.; Rosen, N.; Hartl, F. U.; Pavletich, N. P. Crystal structure of an hsp90-geldanamycin complex: targeting of a protein chaperone by an antitumor agent. *Cell* **1997**, *89*, 239–250. (b) Ali, M. M. U.; Roe, S. M.; Vaughan, C. K.; Meyer, P.; Panaretou, B.; Piper, P. W.; Prodromou, C.; Pearl, L. H. Crystal structure of an hsp90-nucleotide-p23/Sba1 closed chaperone complex. *Nature* **2006**, *440*, 1013–1017. (c) Vaughan, C. K.; Gohlke, U.; Sobott, F.; Good, V. M.; Ali, M. M. U.; Prodromou, C.; Robinson, C. V.; Saibil, H. R.; Pearl, L. H. Structure of an hsp90-cdc37-cdk4 complex. *Mol. Cell* **2006**, *23*, 697–707.
- (a) Söti, C.; Rácz, A.; Csérmely, P. A nucleotide-dependent molecular switch controls ATP binding at the C-terminal domain of hsp90. *J. Biol. Chem.* **2002**, *277*, 7066–7075. (b) Allan, R. K.; Mok, D.; Ward, B. K.; Ratajczak, T. Modulation of chaperone function and cochaperone interaction by novobiocin in the C-terminal domain of hsp90. Evidence that coumarin antibiotics disrupt hsp90 dimerization. *J. Biol. Chem.* **2006**, *281*, 7161–7171.
- (a) Marsaud, V.; Gougelet, A.; Maillard, S.; Renoir, J. M. Various phosphorylation pathways, depending on agonist and antagonist binding to endogenous estrogen receptor alpha (ERalpha), differentially affect ERalpha extractability, proteasome-mediated stability, and transcriptional activity in human breast cancer cells. *Mol. Endocrinol.* **2003**, *17*, 2013–2027.
- (a) Mimnaugh, E. G.; Chavany, C.; Neckers, L. Polyubiquitination and proteasomal degradation of the p185<sup>c-erbB-2</sup> receptor protein-tyrosine kinase induced by geldanamycin. *J. Biol. Chem.* **1996**, *271*, 22796–22801. (b) Münster, P. N.; Marchion, D. C.; Basso, A. D.; Rosen, N. Degradation of HER2 by ansamycins induces growth arrest and apoptosis in cells with HER2 overexpression via a HER3, phosphatidylinositol 3'-kinase-AKT dependent pathway. *Cancer Res.* **2002**, *62*, 3132–3137.



- (22) Marx, C.; Yau, C.; Banwait, S.; Zhou, Y.; Scott, G. K.; Hann, B.; Park, J. W.; Benz, C. C. Proteasome-regulated ERBB2 and estrogen receptor pathways in breast cancer. *Mol. Pharmacol.* **2007**, *71*, 1525–1534.
- (23) Caplan, A. J.; Mandal, A. K.; Theodoraki, M. A. Molecular chaperones and protein kinase quality control. *Trends Cell Biol.* **2007**, *17*, 87–92.
- (24) Stepanova, L.; Leng, X.; Parker, S. B.; Harper, J. W. Mammalian p50Cdc37 is a protein kinase-targeting subunit of Hsp90 that binds and stabilizes Cdk4. *Genes Dev.* **1996**, *10*, 1491–1502.
- (25) Vogel, C. L.; Cobleigh, M. A.; Tripathy, D.; Gutheil, J. C.; Harris, L. N.; Fehrenbacher, L.; Slamon, D. J.; Murphy, M.; Novotny, W. F.; Burchmore, M.; Shak, S.; Stewart, S. J.; Press, M. Efficacy and safety of Trastuzumab as a single agent in first-line treatment of HER2-overexpressing metastatic breast cancer. *J. Clin. Oncol.* **2002**, *20*, 719–726.
- (26) Wellbrock, C.; Karasarides, M.; Marais, R. The Raf proteins take centre stage. *Nat. Rev. Mol. Cell Biol.* **2004**, *5*, 875–885.
- (27) Nicholson, R. I.; Hutcheson, I. R.; Hiscox, S. E.; Knowlden, J. M.; Giles, M.; Barrow, D.; Gee, J. M. W. Growth factor signalling and resistance to selective oestrogen receptor modulators and pure anti-oestrogens: the use of anti-growth factor therapies to treat or delay endocrine resistance in breast cancer. *Endocr. Relat. Cancer* **2005**, *12*, S29–S36.
- (28) Bratton, S. B.; MacFarlane, M.; Cain, K.; Cohen, G. M. Protein complexes activate distinct caspase cascades in death receptor and stress-induced apoptosis. *Exp. Cell Res.* **2000**, *256*, 27–33.
- (29) Jänicke, R. U.; Sprengart, M. L.; Wati, M. R.; Porter, A. G. Caspase-3 is required for DNA fragmentation and morphological changes associated with apoptosis. *J. Biol. Chem.* **1998**, *273*, 9357–9360.
- (30) Liang, Y.; Yan, C.; Schor, N. F. Apoptosis in the absence of caspase 3. *Oncogene* **2001**, *20*, 6570–6578.
- (31) Germain, M.; Affar, E. B.; D', Amours, D.; Dixit, V. M.; Salvesen, G. S.; Poirier, G. G. Cleavage of automodified poly(ADP-ribose) polymerase during apoptosis. *J. Biol. Chem.* **1999**, *274*, 28379–28384.
- (32) Hooper, D. C.; Wolfson, J. S.; McHugh, G. L.; Winters, M. B.; Swartz, M. N. Effects of novobiocin, coumermycin A1, clorobiocin, and their analogs on *Escherichia coli* DNA gyrase and bacterial growth. *Antimicrob. Agents Chemother.* **1982**, *22*, 662–671.
- (33) Hickman, J. A. Apoptosis and tumorigenesis. *Curr. Opin. Genet. Dev.* **2002**, *12*, 67–72.
- (34) (a) Gagne, D.; Balaguer, P.; Demirpence, E.; Chabret, C.; Trousse, F.; Nicolas, J. C.; Pons, M. Stable luciferase transfected cells for studying steroid receptor biological activity. *J. Biolumin. Chemilumin.* **1994**, *9*, 201–209. (b) Balaguer, P.; Francois, F.; Comunale, F.; Fenet, H.; Boussioux, A. M.; Pons, N.; Nicolas, J. C.; Casellas, C. Reporter cell lines to study the estrogenic effects of xenoestrogens. *Sci. Total Environ.* **1999**, *233*, 47–56.

JM0707774